Figure S1 Related to Figure 1. Detection of sites of phosphorylation on WC-1 and WC-2 by mass spectrometry. **A** Phosphosites on WC-1 identified by MS/MS at DD15 when the WCC is active, DD24 when the WCC is inactive, LP15' (light pulse for 15 min) when the WCC undergoes maximal light-dependent phosphorylation, and LL (constant light) when the WCC constantly induces FRQ expression. In the table, each yellow box represents a phosphorylation site observed and the number in each yellow box shows the number of times the phosphosite has been detected. Numbers on the left of the phospho-map indicate the position of the WC-1 residue(s) that is phosphorylated. Previously reported phosphosites are underlined. Numbers above each column indicate the number of biologically independent samples used to collect mass spec data. **B** Phosphosites on WC-2 identified by MS/MS under the same four conditions used in **A**. As before, each yellow box represents a phosphorylation site observed and the number in each yellow box shows the number of times the phosphosite has been detected. Numbers on the left of the phospho-map indicate the position of the WC-2 residue(s) that is phosphorylated. The previously reported phosphosite is underlined. **C** Mass spectrometry coverage of WC-1 and WC-2 by trypsin or/and protease K. Regions in black were directly sequenced by MS/MS while no peptides were recovered for the blank regions. Recent MS/MS assays have covered some of the 33 Ser/Thr on WC-1 originally undetected by MS/MS (Figure 1B), although no additional phosphosites have been identified on these residues. Additionally, two small N-terminal regions of WC-2 were not covered by MS/MS, and these contain WC-2 S2, S10, S11, S22, S26, S30, T34, T38, and T42. However, by the time WC-2^{15pA} was made we had also established the Phos-tag system and had shown that none of these were ever phosphoryated

(Figures 4D, S6B). For this reason we never made S/T to A mutants for any of these sites and they are not shown as “missed by MS” in Figures 1 or 2.

Figure S2 Related to Figure 1. Quantitative Analysis of WC-1 phosphorylation. WC-1 purified from a culture grown in the dark for 24 hr was subject to protease digestion and labeled by reductive dimethylation (See Methods). M* refers to oxidized methionine.

Figure S3 Related to Figure 1. **A** Activity of the WCC in the core circadian oscillator of the strains shown was assayed over 5 days using a *frq C-box*-luciferase transcriptional reporter as described in STAR Methods. Raw data, neither smoothed, background subtracted, nor detrended, are shown. Time is shown in hours on the X-axis. Different colored lines represent three replicates and the period length ± SD is shown. The three panels show loss of rhythmicity in strains whose genotype is listed on the figure. In these and similar figures, note differences in the vertical scale bars, which were adjusted so each data panel fit within the same space in the figure, and compare these to the scale bar in the control in Figure 1. The vertical axes show relative light levels reflecting WCC activity measured as a function of time; because inocula were the same and because the sequence differences in WC-1 and WC-2 did not result in measurable changes in growth, the amount of bioluminescence provides a semiquantitative measure of the amount of WCC activity *in vivo*. **B** Western blot analysis showing that the WC-1 level in *wc*-1^{113A} and *wc*-1^{80A} is extremely low (upper left and lower blot), alanine mutations at aa 363, 373, 390, and 525 alone severely reduce the WC-1 level (upper right blot), and FRQ and WC-1 levels in *wc*-1^{109A} and *wc*-1^{77A} are increased as compared to *wc*-1^{113A} and *wc*-1^{80A}. Protein levels were assayed at DD0 (constant light), DD16 (when new FRQ peaks in the WT), and DD24 (when old FRQ is extensively

phosphorylated in the WT). **C** WC-1^{113A} and WC-1^{80A} are less stable than that in WT (upper blot). Strains of the genotype shown were grown for 16 hrs in the dark prior to addition of cycloheximide (CHX) to 40 µg/ml. Cultures were harvested at the times shown and proteins visualized by Western blotting. **D** Multiple phosphosite mutations do not abrogate the interaction of WC-1 with WC-2. Cultures were grown in constant light, and extracts used for Western blot analysis of co-immunoprecipitations showing the protein levels of FRQ, WC-1, WC-2 and FRH in WT (328-4), *wc*-1^{V5}, and phosphosite double mutants *wc*-1^{80A}, *wc*-2^{15pA}, and *wc*-1^{113A},*wc*-2^{15pA}. Loadings of protein extracts were adjusted as shown to provide a scale for estimating amounts and differences between strains.

Figure S4 Related to Figures 1E and 2. **A** Western blot analysis showing the protein levels of FRQ, WC-1, WC-2, and luciferase in *frq C-box*-luc-transformed WT (661-4a), *wc*-2^{15pA}, and *wc*-2^{15pD} as indicated. In these strains, luciferase is driven by the *frq C-box* at the *his*-3 locus as a transcriptional reporter of the WCC activity. **B** Overt rhythmicity in WT and in the *wc*-2 mutant WC-2^{15pA} in which all confirmed phosphosites on WC-2 are converted to Ala; WC-1 is not mutated. **C** (covering multiple pages) Detailed circadian phenotypic analysis of WCC activity over 5 days in WC-1 and WC-2 phosphosite mutants measured by *frq C-box*-luciferase transcriptional fusion reporter assay as described in STAR Methods. These data underlie the estimates of rhythmicity used to localize regions required for circadian feedback as noted in Figure 2 **A** and **B.** Raw data, neither smoothed, background subtracted, nor detrended, are shown. As in Figure S3A, because the amount of light provides a semiquantitative measure of the amount of WCC activity *in vivo*, in this assay, for instance, the arrhythmic strain bearing

wc-1$^{S971A,\ S988A,\ S990A,\ S994A,\ S995A}$, *wc*-2^{15pA} produces about 5X more light than the rhythmic strain *wc*-1$^{S971A,\ S988A,\ S990A,\ S994A,\ S995A}$. **D** Race tube analyses of wild-type (WT) and *wcc* mutants as shown. Pictures of replicate tubes are shown, and the vertical black lines in race tubes depict daily growth fronts of the strains. 328-4 (*ras*-1^{bd} *A*) served as the WT. Bar graph shows period estimates from the four strains as marked; error bars ± SD, n=3. **E** Histogram of period data for WCC mutant (S-A substitution and deletion) strains from Table S1, meant to provide context for judging how deviant various period lengths are from WT. The box encloses the region of WT period lengths ± 2 Std Dev.

Figure S5 Related to Figure 4. Analysis of *in vitro* phosphorylation of WC-1 and WC-2 confirms that a single phosphoevent on either WC-1 or WC-2 can be resolved by the 149:1 gel system containing 20 µl phos-tag. **A** In WC-1^{STYtoA} all Ser, Thr, and Tyr residues have been mutated to Ala; the protein is tagged with V5 at its C-terminus. In this context, a single Ser as indicated was added back , so that only one site in the protein can be phosphorylated. WC-1 was isolated using V5 antibody from the lysate of these strains cultured in the dark for 16 hr as described in Methods. The washed beads were incubated with 50 µL of protein kinase buffer (NEB) at 99°C for 5 min and the mixture was immediately transferred onto ice to dissociate WC-1 from the beads. Kinases were chosen from the list of predictions based on consensus sites shown in Table S3. 2 µl of kinases as indicated and 2.5 µl of 10 mM ATP were added to the mixture and incubated at 30°C for 1 hr. Proteins in the lysate were separated by phos-tag gels as described in Methods and analyzed by Western blotting using anti V5. Phosphorylation of S94, S831, S971, or S1015 in *wc*- 1^{STYtoA} was revealed by the *in*

vitro kinase assay using kinases as indicated. **B** Similar to the case for panel A, *in vitro* kinase assays were performed with WC-2$^{STYtoA,\ A118S}$ or WC-2$^{STYtoA,\ A324S}$ respectively with the indicated kinase and in the presence of ATP.

Figure S6 Related to Figure 4. Phos-tag gels confirm *in vivo* phosphorylation of WC-1 and WC-2 at selected residues. **A** Replicate controls demonstrating an absence of WC-1 phosphorylation in WC-1^{113A} and WC-1^{109A}, and an absence of WC-2 phosphorylation in WC-2^{15pA}. Cultures of the indicated genotypes were harvested after the number of hours shown in the dark, treated or not with Lambda phosphatase as shown (see Methods), and examined by Western blotting using 6.5% acrylamide gels containing 149:1 acrylamide:bisacrylamide and 20 µM phos-tag (see Methods). **B** In the context of WC-1^{113A} (top) or WC-1^{15pA} (bottom), individual phosphorylatable Ser were added back into the proteins as indicated. Cultures bearing the modified alleles were cultured in darkness for 24 hrs, lysates prepared, treated with lambda phosphatase as indicated, and analyzed by Western blotting using phos-tag gels as in **A**.

Figure S7. Related to Figures 4 and 5. **A** FRQ promotes phosphorylation of certain residues in WC-1 and WC-2. **A** Western blot showing complete loss of phosphorylation in *wc*-1^{113A}, and FRQ-induced phosphorylation in WC-1$^{113A\ A603\text{-}966p\ back}$ (repeated from Figure 4) and also in regions N-terminal or C-terminal to the WC-1 ZnF as shown. As in Figure 4, Western blots were performed using the 149:1 gel containing 20 µl phos-tag (See Methods). In the context of WC-1^{113A}, all Ser/Thr from aa 603 to aa966, or aa 852 to aa966, or aa996 to aa1023, or aa996 to aa1167 were returned to normal sequence and thus available for phosphorylation, whereas all other WC-1 Ser/Thr remained converted to Ala. These strains were either backcrossed to introduce Δ*frq* or

transformed with *qa*-2 promoter-driven *frq* at the *csr* locus. To cultures in constant light, inducer (10^{-2} M QA) was added and the cultures immediately moved to dark for 16 hr. Phos-tag Western blots as in **A** are shown. **Right panel** In the context of unphosphorylatable WC-1^{113A}, Ser was restored at aa1015, and the allele placed in a Δ*frq* or QA-inducible *frq* background and assayed for WC-1 phosphorylation**. B** (Related to Figure 5**A**) Race tube assays of *wc*-1 phosphomutants as indicated showing deterioration of overt circadian output in some phosphosite mutants surrounding the essential region. The strains were cultured on standard 0.1% glucose race tube medium in the light at 25°C overnight (12 to 16 h) prior to growth in the dark at 25°, except for the WC-$1^{1\text{-}970\&996\text{-}1167A}$ race tubes that were here run on 0.01% glucose to confirm that while nutrition can clarify the overt rhythm to some extent it remains less robust that WT. Images of replicate race tubes are displayed, and the vertical lines in race tubes depict the growth fronts of the strains every 24 h. **C** (related to Figure 5 B) Western blot examining effects of loss of phosphorylation in restricted regions of WC-1, showing reduced levels of WC-1 and WC-2 with increased FRQ in constant light (L), DD16 (~CT4, subjective morning), and DD24 (~CT14, subjective evening). This figure shows the entire gel from the right hand panel of Figure 5B. Mutation of WCC residues essential for feedback repression has dramatic effects on WCC and FRQ levels; the level of FRQ is inversely proportional to the amount of WCC. Experimental conditions as in Figure 5B.

Figure S8 Related to Figure 4. Repression of WCC activity by FRQ is not through disruption of the interaction between WC-1 and WC-2. **A** Immunoprecipitation assays

using V5 antibody showing (left) that over-expression of FRQ does not disrupt the interaction between WC-1 and WC-2. WC-1^{V5} and WC-1^{V5}, Δ*frq* serve as the positive and negative controls, respectively. A *wc*-1 allele tagged with the V5 epitope tag at its C-terminus was placed at its resident locus in three genetic backgrounds, WT, Δ*frq*, and the inducible Δ*frq*,*qa*-2*frq* (as two biologically distinct replicate strains). Following immunoprecipitation of WC-1 via the V5 tag, levels of WC-1, WC-2 and FRQ were monitored by Western Blot. (right) Immunoprecipitation assays using V5 antibody showing that the ability of WC-1 and WC-2 to be phosphorylated at the core sites required for repression does not impact their ability to interact and form the WCC, and that phosphor-mimetics at those sites also do not impact WCC formation. The immunoprecipitation assays were carried out as described in STAR Methods. **B** A translational fusion, in which the WC-2 ORF tagged with V5 as shown was placed in frame immediately after the WC-1 ORF (upper left panel), was inserted into the resident *wc*-1 locus in either a WT of a Δ*wc*-2 background. The WC-1-WC-2 fusion protein is able to sustain a normal circadian rhythm based on luciferase assays (lower panels); however, the amplitude of the oscillator is dampened, especially when there is an additional copy of *wc*-2, with a resulting deterioration of the overt rhythm as revealed by race tube assays (upper right). **C** Western blot analysis showing protein levels of WC-1, WC-2, FRQ, and FRH in the *wc*-1-*wc*-2 fusion mutant.

Figure S9 (covering multiple pages) Related to Figure 6. Identification and analysis of novel direct targets of the WCC and analysis of other WCC targets within the first step of circadian output. **A** Shown is a screenshot of GBrowse of data from a series of ChIP-seq experiments using anti-WC-2. For each of twelve genes, the top shows the gene

map within this region, with the pertinent transcription unit circled. The coding region is in dark blue and the 5' and 3' untranslated regions are in yellow; gaps represent introns, and the arrow points in the direction of transcription. Vertically below this are Δ*wc*-1 (negative control for WCC binding) and binding assessed at 4 hr intervals from DD4 to DD32. The peak of WCC binding within the promoter of each gene is marked by the box and arrows indicate the primer pairs (Table S5) used to detect the region for qPCR in panel **B**. Circadian changes in the level of WCC binding as reflected in the peak heights are plain because the scale bars, which provide the absolute level of binding, and are the same within each panel although they are different between panels. **B** qPCR data using primers (Table S5) to assess binding of WC-2 to the sites marked in panel **A** in WT and four mutants as shown, revealing that mutant strains that have lost circadian repression within the feedback loop are also altered for binding related to circadian output. Binding was assessed at DD16 (~CT4, subjective morning) and DD24 (~CT14, subjective evening). Error bars are SEMs (n=3)

Table S1 Related to Figure 1. Circadian periods of the *wcc* phosphomutants by race tube assays.

Table S2 Related to Figure 1. Periods of circadian rhythms in Ser/Thr/Tyr to alanine mutants of *wc*-1 or *wc*-2 on race tubes.

Table S3 Related to Figures 4 and S5. Prediction (with 90% prediction specificity) of kinases responsible for important phosphosites on WC-1 and WC-2 by KinasePhos (http://kinasephos.mbc.nctu.edu.tw/).

Table S4 Related to Figures 2 and S4C. Circadian period of the *wcc* mutants as reported by the *frq* promoter-driven *luciferase* gene assay. Briefly, cultures were

examined by CCD camera with a 10 min exposure every hour for five days, data extracted as described (Larrondo et al., 2012), and period length calculated using custom the Matlab software.

Table S5 Related to Figures 3, 5, and S6. Primers sets used in Figure 3, Figure 5 and Figure S6

A

Replicates	3	4	2	2
Sites	LL	DD24	LP15	DD15
S8	3		10	4
S11	2		13	6
S92	3		8	2
S94	1	1	1	1
S92 or S94			2	
S111	18	4		3
T120	1			
S124	6			4
Y198	5			2
Y198 or S200			5	5
S200	9	1	10	7
T214		1		
T217		1		
S227	2			
S231	1			
S229 or S231				1
S234	13	6	17	9
T238	5	1	7	3
S264			1	
T275			5	
T279	1			
T287	4			1
S302				1
S307			3	
S307 or T308			6	1
T308 or T311			1	
T308			7	1
T312		1		
S315	6		11	5
S319			2	
S319 or T321			1	
T324		1		
S334	4	1	4	
S334 or T336			2	1
T336	2			
T340	1		2	
T345	2			
S346	1			
T347	1			
S349		1		
S363	1		2	
Y373		1		
Y525 or T526			2	
T526	1			
S528	1		2	
T536	4	1		
S602	1			
S748		1		
T755		1		
S809		1		
T819	1			1
S824	20	2	33	4
S831	61	14	103	31
T838			1	
S840	3			1
S840 or S842	1			
S842	3			
S852, S854 or S855	2		2	
S854	1	1		
S855		2		
S857	1	2	1	
S866 or S867			1	
S867		1		
S892	1		1	
S971		10		
S985		1		
S988	2	12	10	2
S990	12	31	21	10
S992	2	4	5	3
S994		8	3	1
S995	3	6	5	2
S1005	10	19	6	4
S1007		2		
T1008		2		
T1009		1		
T1012	1	1	1	
S1015	15	45	16	10
S1017			1	
S1021		1		
T1023		1		
T1068		1		
S1071	4	1	2	
S1074	2	4	9	3
S1134		1		
S1142			1	

B

Replicates	3	4	2	2
Sites	LL	DD24	LP15	DD15
S82	1		1	
S118	1	3	4	
T136		2		
S233		1		
S324		1		
S331		3		
T339	15	5	1	
S341	2	1		
T344	1	1		
T346		1		
S394	1	1		
T428		2		
T429		1		
S433	13	27	8	2
T435	1	6		

C

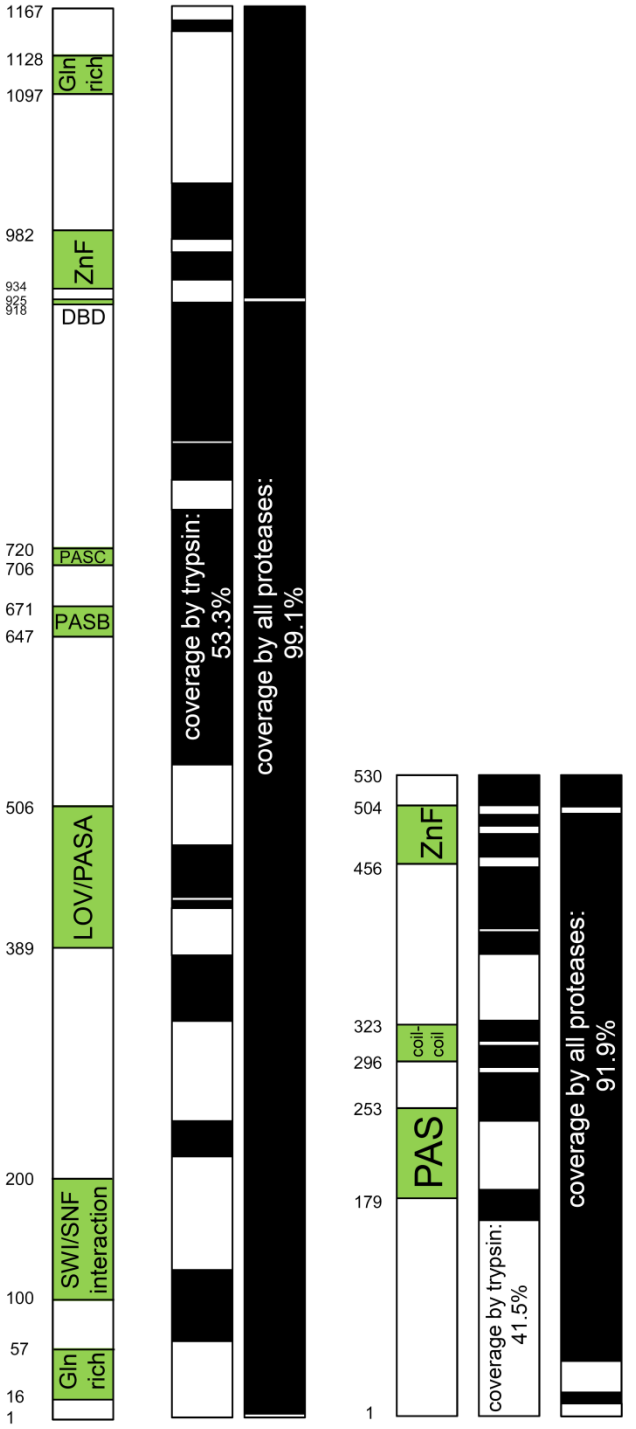

Figure S1

sequence	modsites	occupancy	percentage occupancy
M.T#PAMTPGVSNF.A	T283	low	3.39
H.VLS#LKGL.F	S593	low	0.03
E.S#RAEFGR.T	S748	high	99.90
K.NM*S#PGGVPLSPM*K.G	S824	low	24.82
K.NM*SPGGVPLS#PM*K.G	S831	low	24.82
K.QTGRVS#PR.T	S971	high	99.90
K.KS#NS#PSHSSPLHR.E	S988:S990	high	99.09
K.KSNS#PSHSSPLHR.E	S990	high	99.09
K.KSNSPS#HSSPLHR.E	S992	high	99.09
K.SNS#PSHSSPLHR.E	S990	high	99.90
K.SNS#PSHSS#PLHR.E	S990:S995	high	99.90
R.EVGNDS#PSTTTATK.N	S1005	high	98.13
R.EVGNDSPSTTTATKNS#PSLR.G	S1015	high	99.38
T.ATKNS#PSLR.G	S1015	high	87.40
T.ATKNS#PSLRGS.S	S1015	high	82.09
T.KNS#PSLR.G	S1015	high	83.51
T.TATKNS#PSLR.G	S1015	high	95.81
T.TAT#KNSPSLR.G	T1012	high	95.81
T.TATKNS#PSLRGS.S	S1015	high	95.35
T.AT#KNSPSLRGS.S	T1012	high	95.35

Figure S2

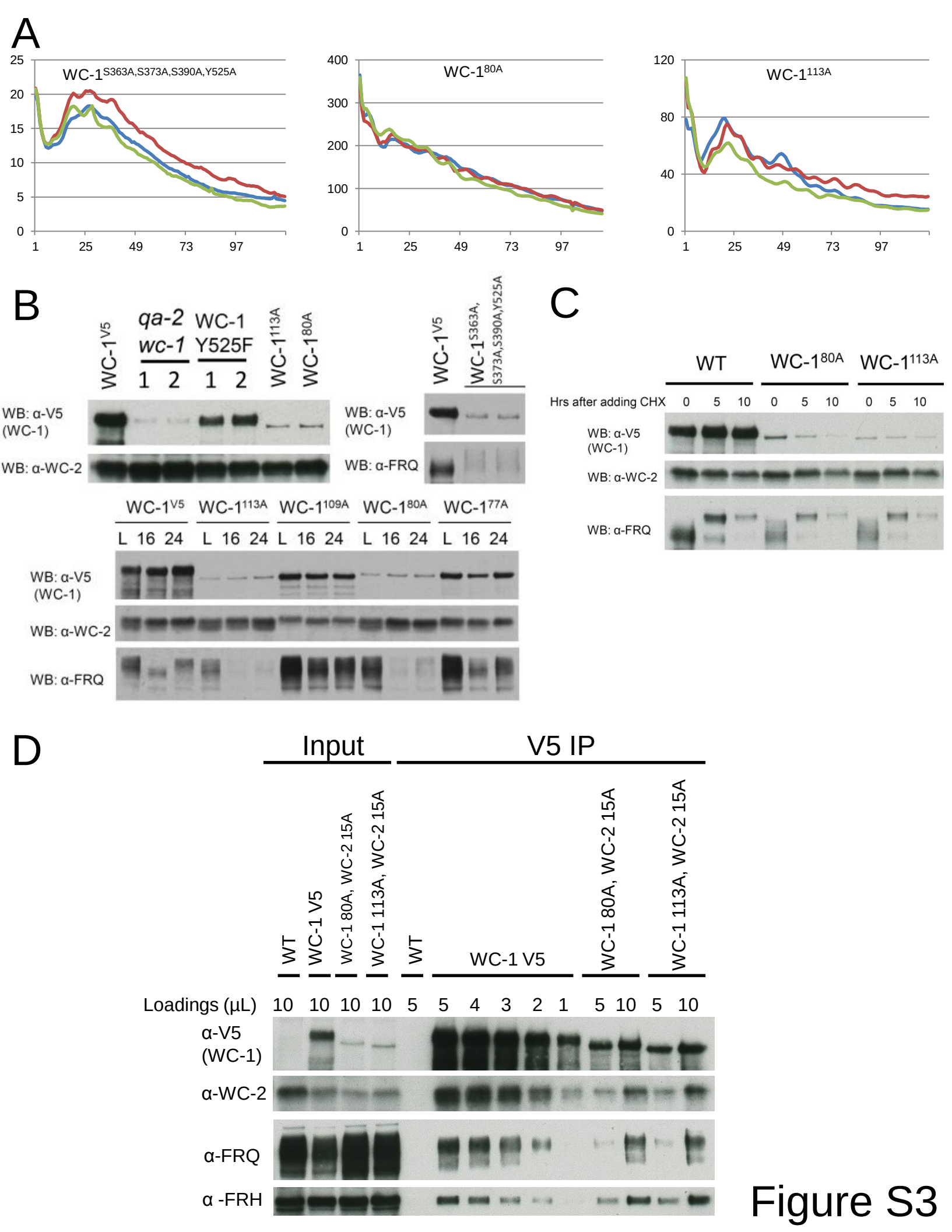
A
WC-1S363A,S373A,S390A,Y525A
WC-180A
WC-1113A
B
WC-1V5
qa-2 wc-1
WC-1 Y525F
1 2 1 2
WC-1113A
WC-180A
WC-1V5
WC-1S363A, S373A,S390A,Y525A
WB: α-V5 (WC-1)
WB: α-WC-2
WB: α-FRQ
WC-1V5
WC-1113A
WC-1109A
WC-180A
WC-177A
L 16 24 L 16 24 L 16 24 L 16 24 L 16 24
C
WT
WC-180A
WC-1113A
Hrs after adding CHX 0 5 10 0 5 10 0 5 10
D
Input
V5 IP
WT
WC-1 V5
WC-1 80A, WC-2 15A
WC-1 113A, WC-2 15A
Loadings (µL) 10 10 10 10 5 5 4 3 2 1 5 10 5 10
α-V5 (WC-1)
α-WC-2
α-FRQ
α -FRH

Figure S3

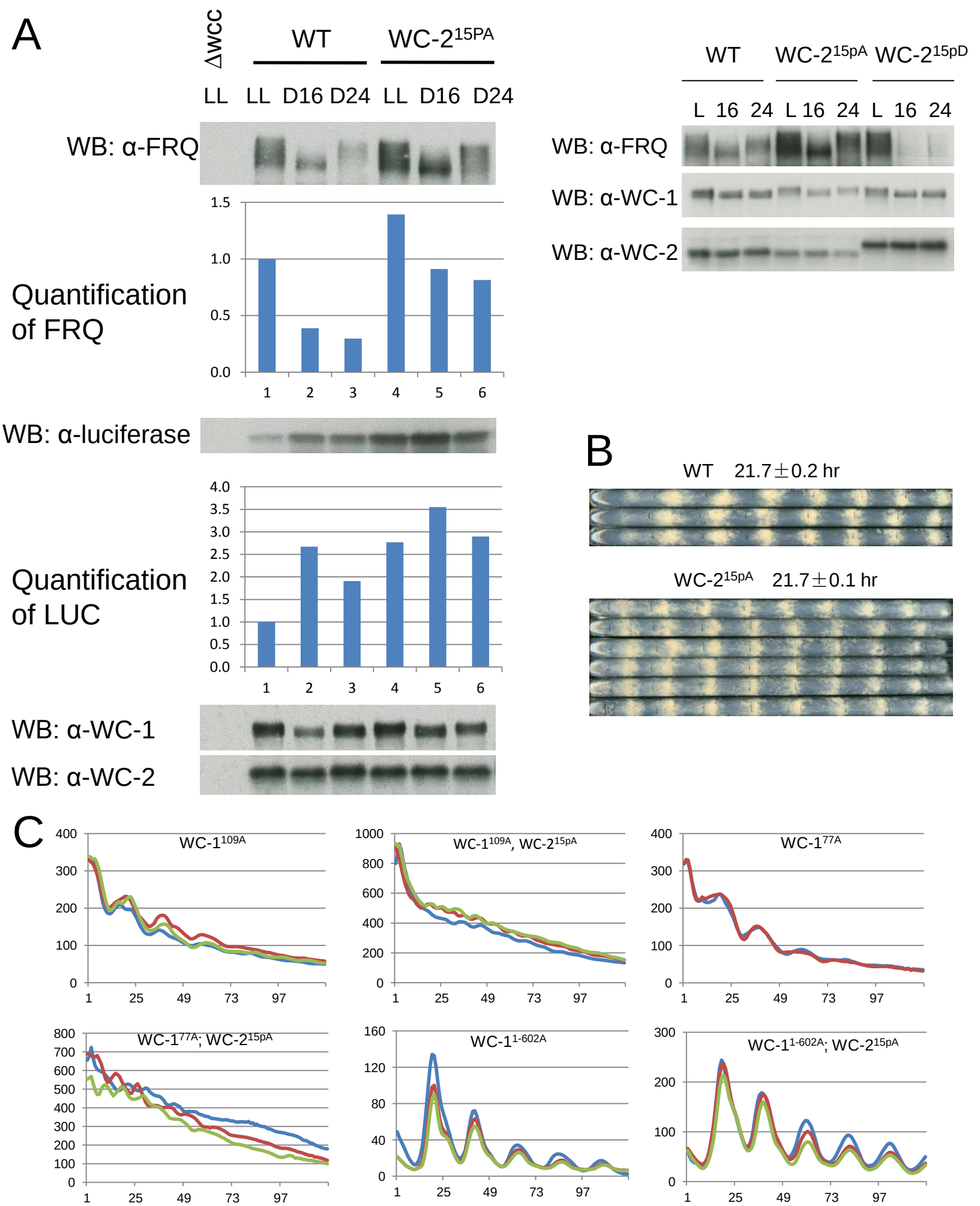
A
ΔWCC
WT
WC-2^15PA
LL LL D16 D24 LL D16 D24
WB: α-FRQ
Quantification of FRQ
WB: α-luciferase
Quantification of LUC
WB: α-WC-1
WB: α-WC-2
WT WC-2^15pA WC-2^15pD
L 16 24 L 16 24 L 16 24
WB: α-FRQ
WB: α-WC-1
WB: α-WC-2
B
WT 21.7±0.2 hr
WC-2^15pA 21.7±0.1 hr
C
WC-1^109A
WC-1^109A, WC-2^15pA
WC-1^77A
WC-1^77A; WC-2^15pA
WC-1^1-602A
WC-1^1-602A; WC-2^15pA

Figure S4

Figure S4 C continued

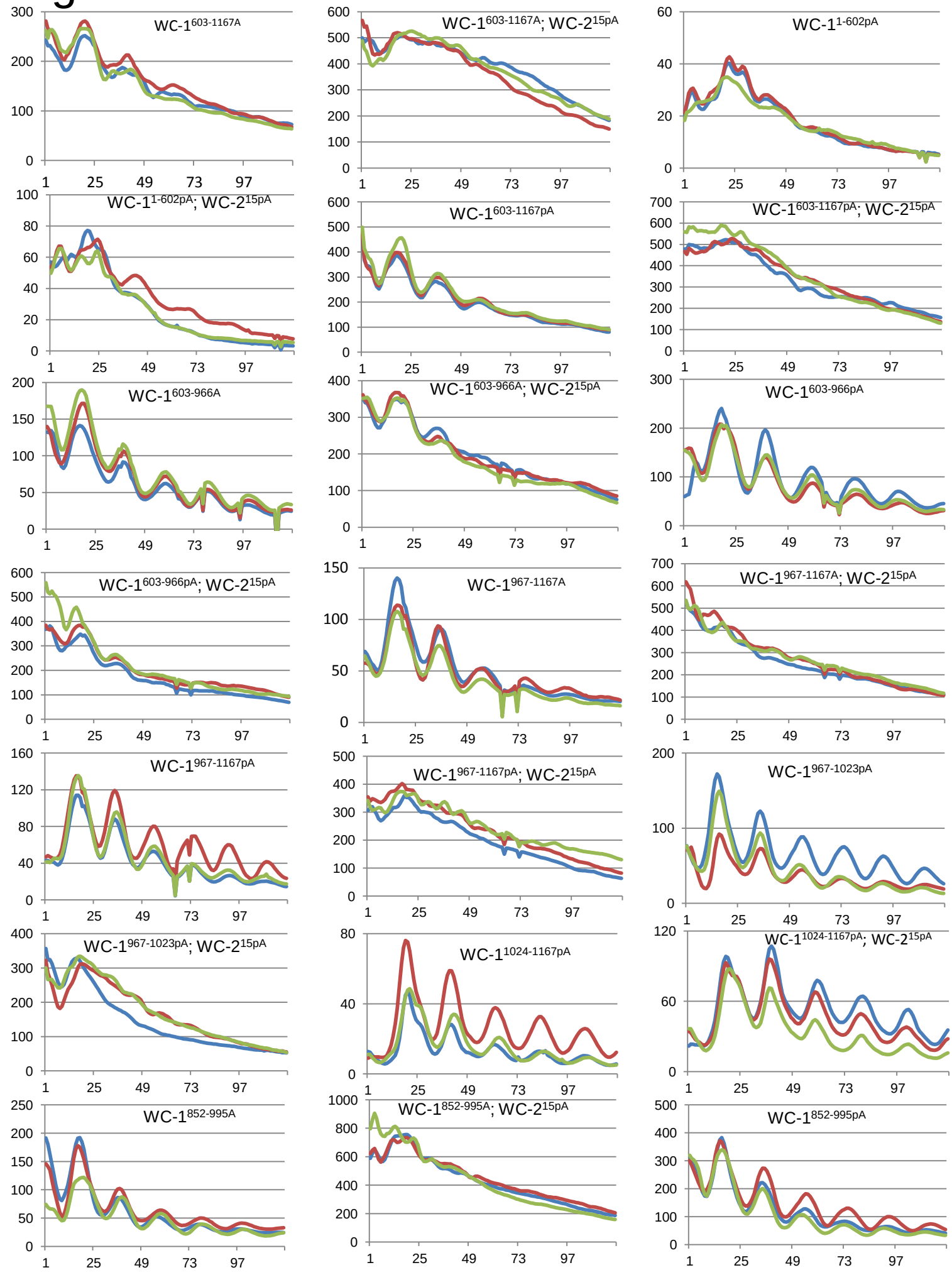

Figure S4 C continued

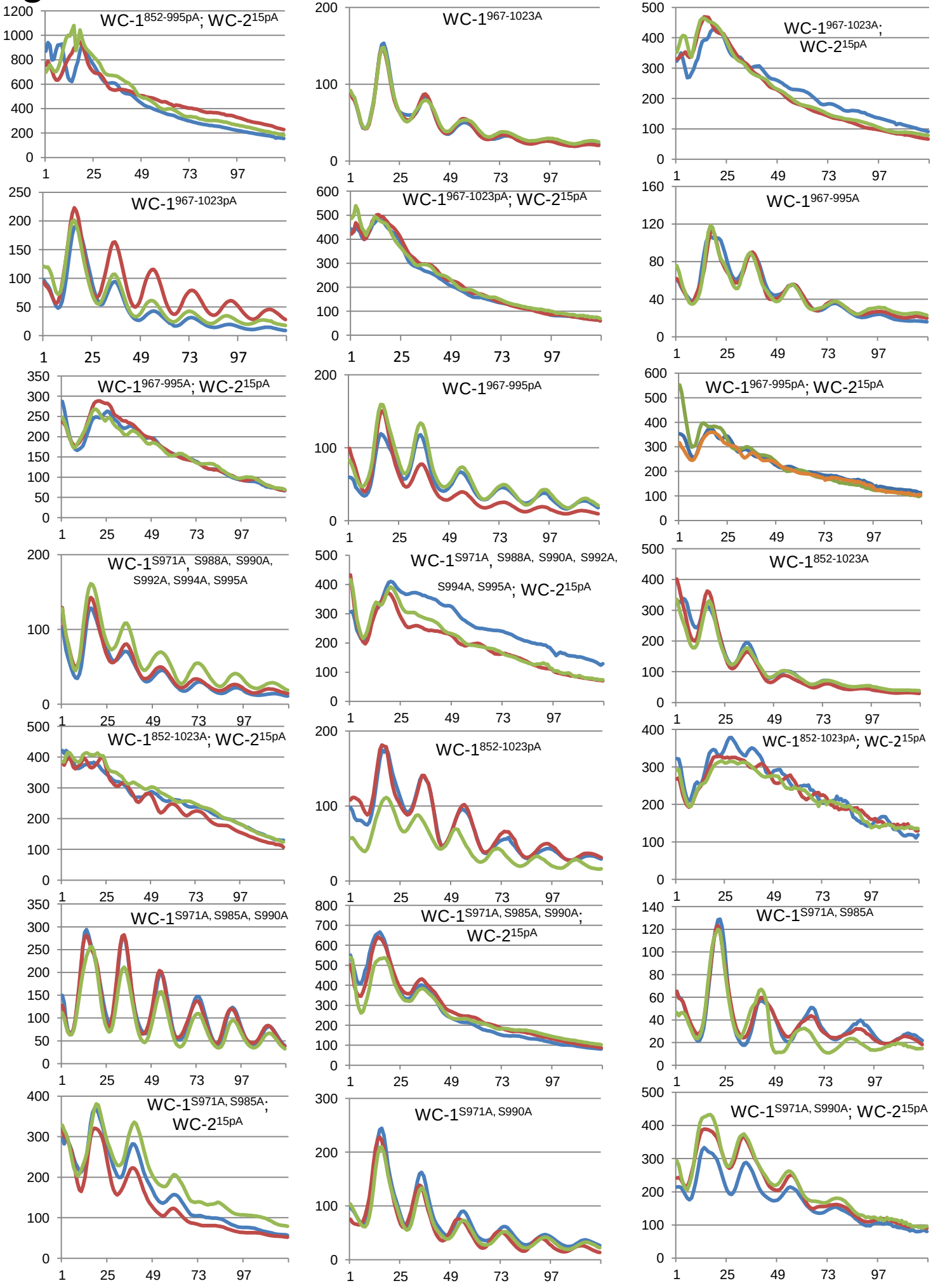

Figure S4 C continued

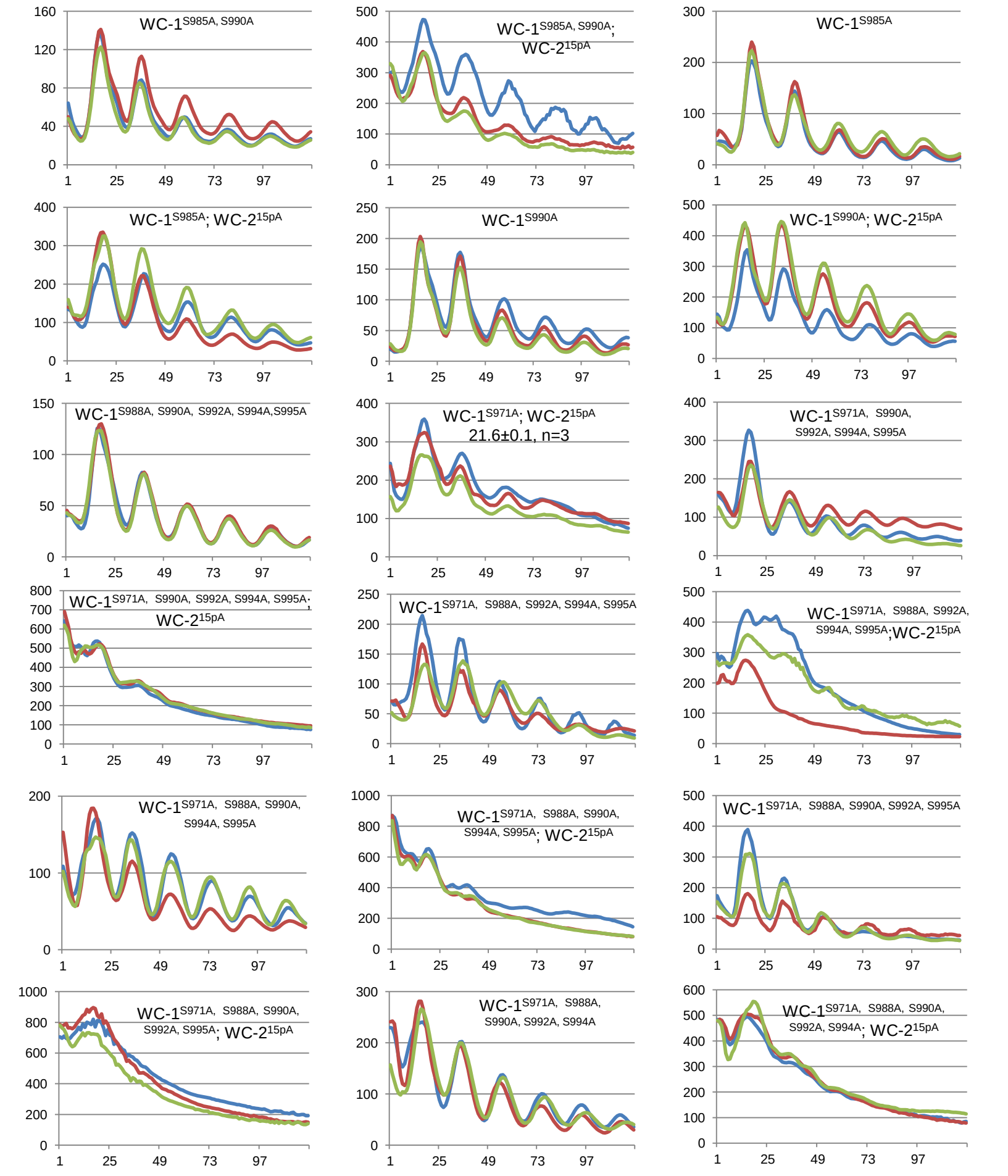

Figure S4 C continued

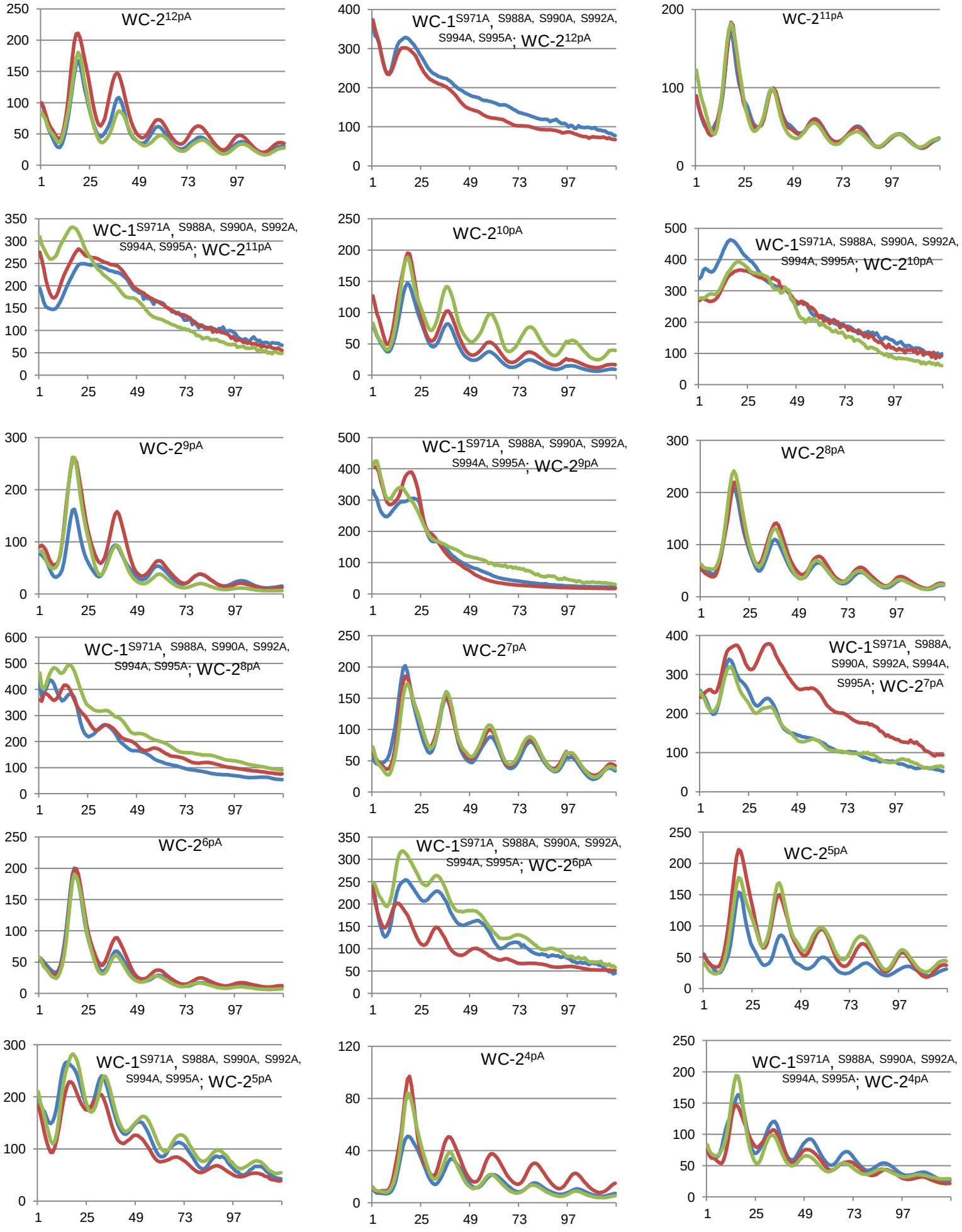

Figure S4 C continued

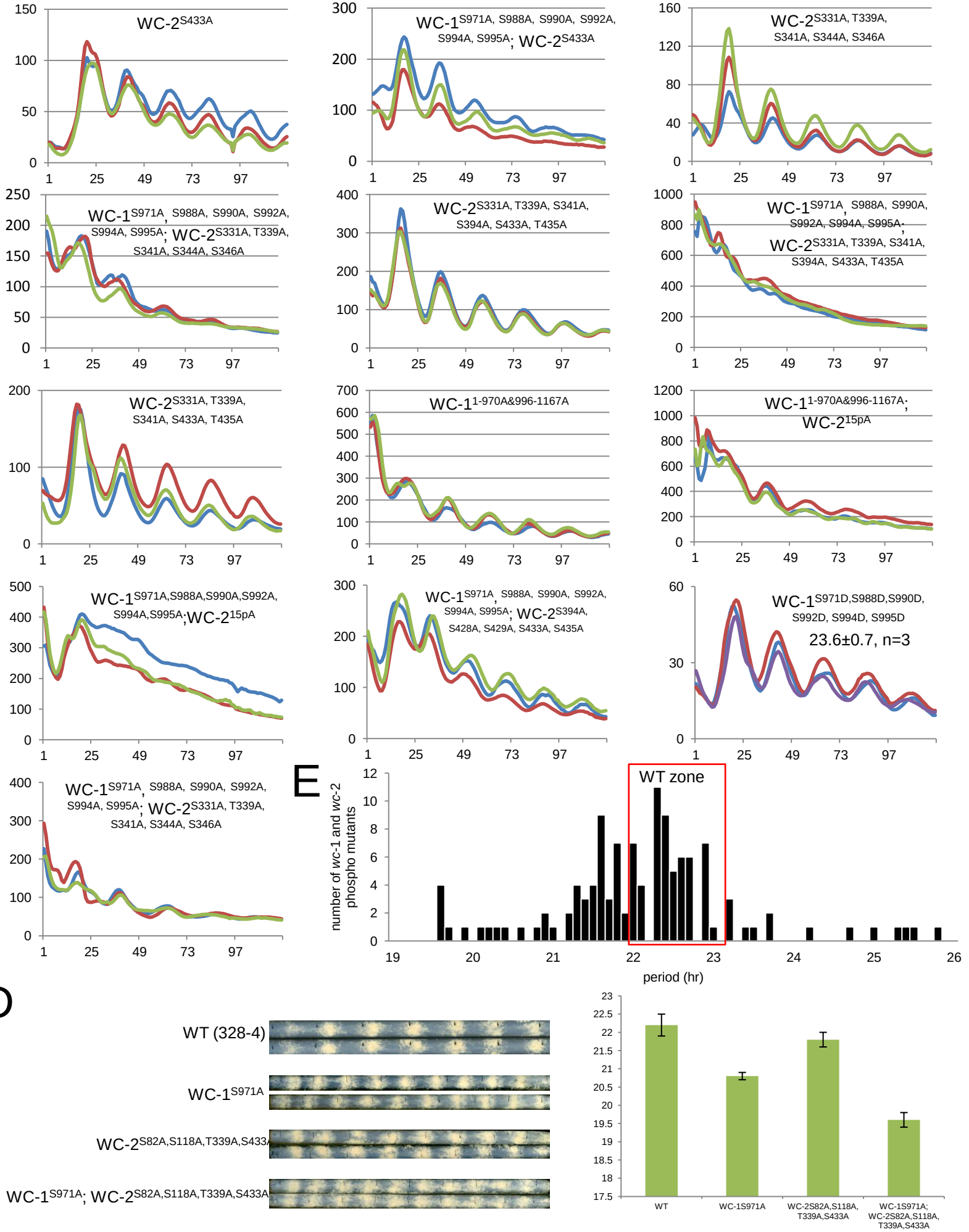

E

D

A

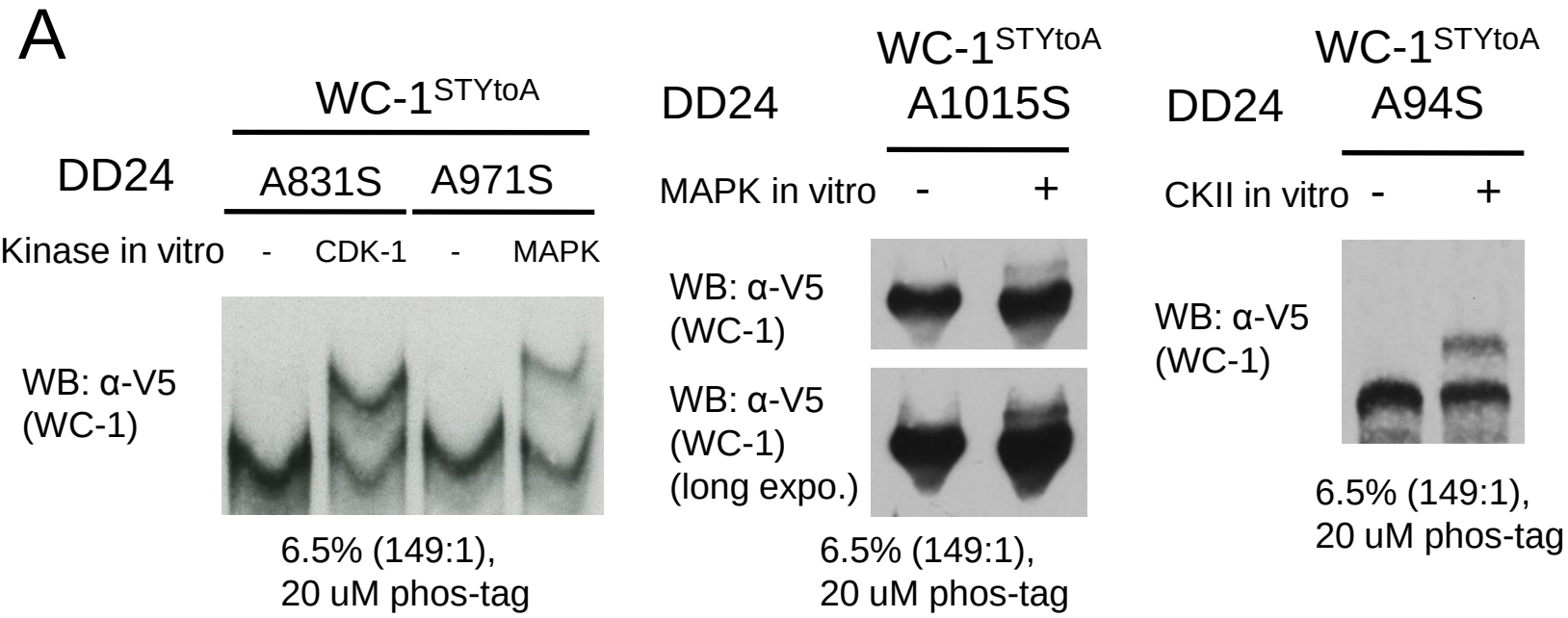
WC-1STYtoA
DD24
A831S
A971S
Kinase in vitro - CDK-1 - MAPK
WB: α-V5 (WC-1)
6.5% (149:1), 20 uM phos-tag
WC-1STYtoA
DD24
A1015S
MAPK in vitro - +
WB: α-V5 (WC-1)
WB: α-V5 (WC-1) (long expo.)
6.5% (149:1), 20 uM phos-tag
WC-1STYtoA
DD24
A94S
CKII in vitro - +
WB: α-V5 (WC-1)
6.5% (149:1), 20 uM phos-tag

B

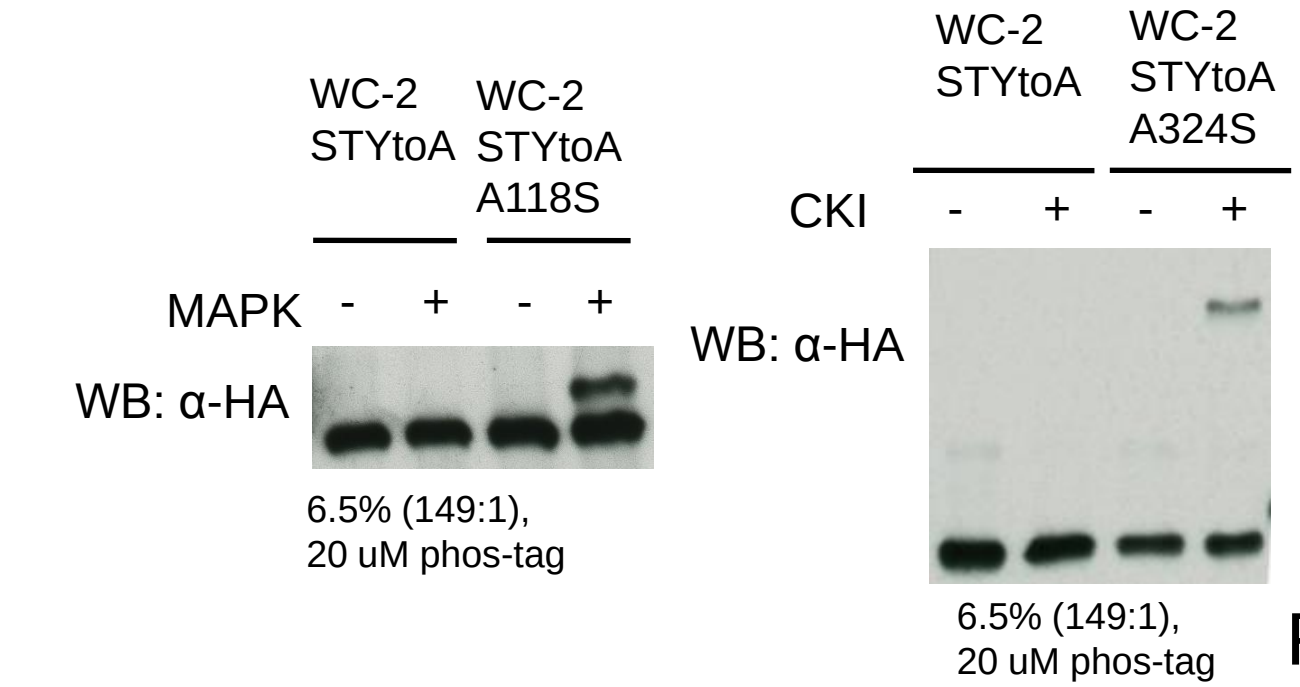
WC-2 STYtoA
WC-2 STYtoA A118S
MAPK - + - +
WB: α-HA
6.5% (149:1), 20 uM phos-tag
WC-2 STYtoA
WC-2 STYtoA A324S
CKI - + - +
WB: α-HA
6.5% (149:1), 20 uM phos-tag

Figure S5

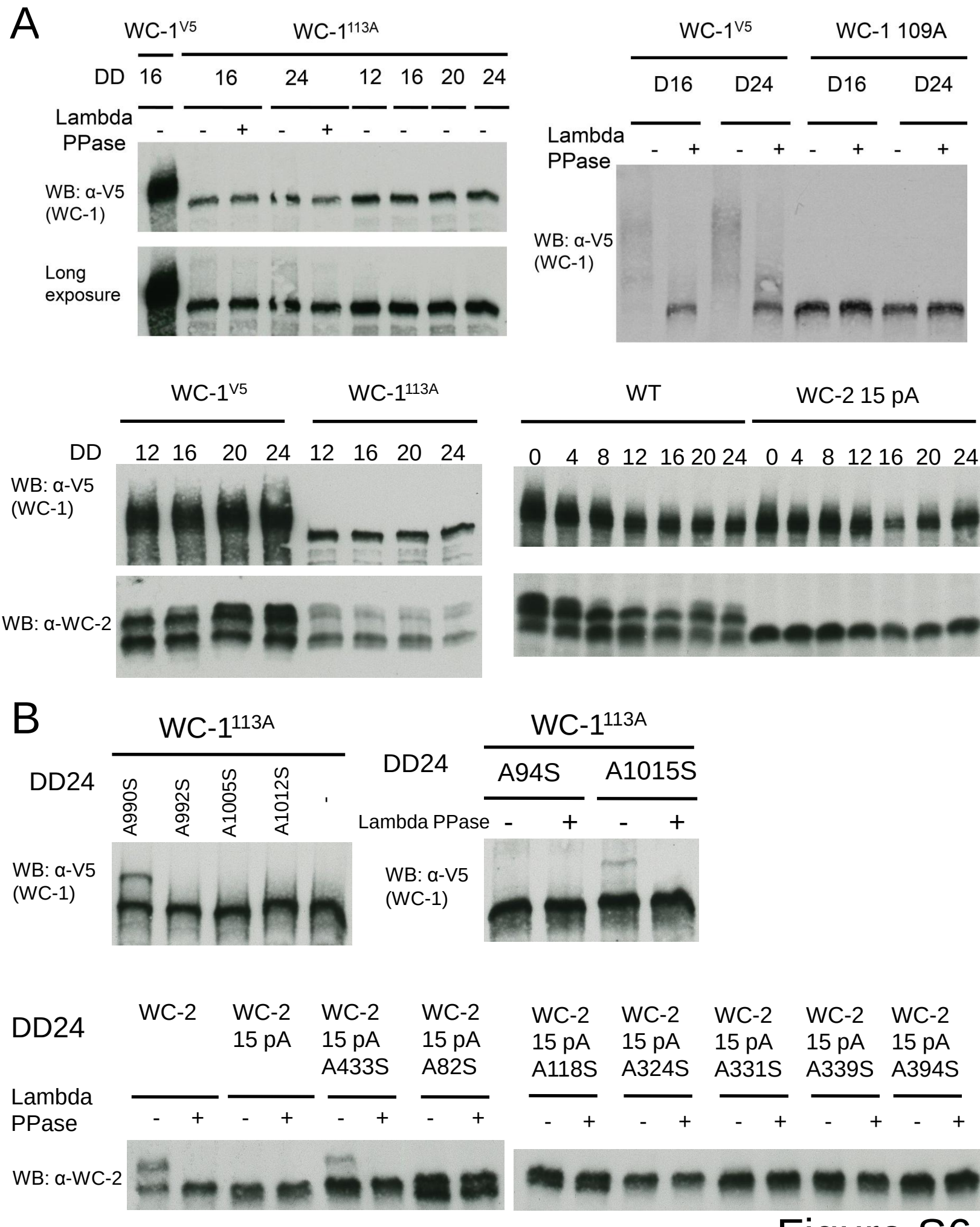
A
WC-1V5
WC-1113A
DD 16 16 24 12 16 20 24
Lambda PPase - - + - + - - - -
WB: α-V5 (WC-1)
Long exposure
WC-1V5
WC-1 109A
D16 D24 D16 D24
Lambda PPase - + - + - + - +
WB: α-V5 (WC-1)
WC-1V5
WC-1113A
DD 12 16 20 24 12 16 20 24
WB: α-V5 (WC-1)
WB: α-WC-2
WT
WC-2 15 pA
0 4 8 12 16 20 24 0 4 8 12 16 20 24
B
WC-1113A
DD24
A990S A992S A1005S A1012S -
WB: α-V5 (WC-1)
WC-1113A
DD24
A94S A1015S
Lambda PPase - + - +
WB: α-V5 (WC-1)
DD24
WC-2
WC-2 15 pA
WC-2 15 pA A433S
WC-2 15 pA A82S
WC-2 15 pA A118S
WC-2 15 pA A324S
WC-2 15 pA A331S
WC-2 15 pA A339S
WC-2 15 pA A394S
Lambda PPase - + - + - + - + - + - + - + - + - +
WB: α-WC-2

Figure S6

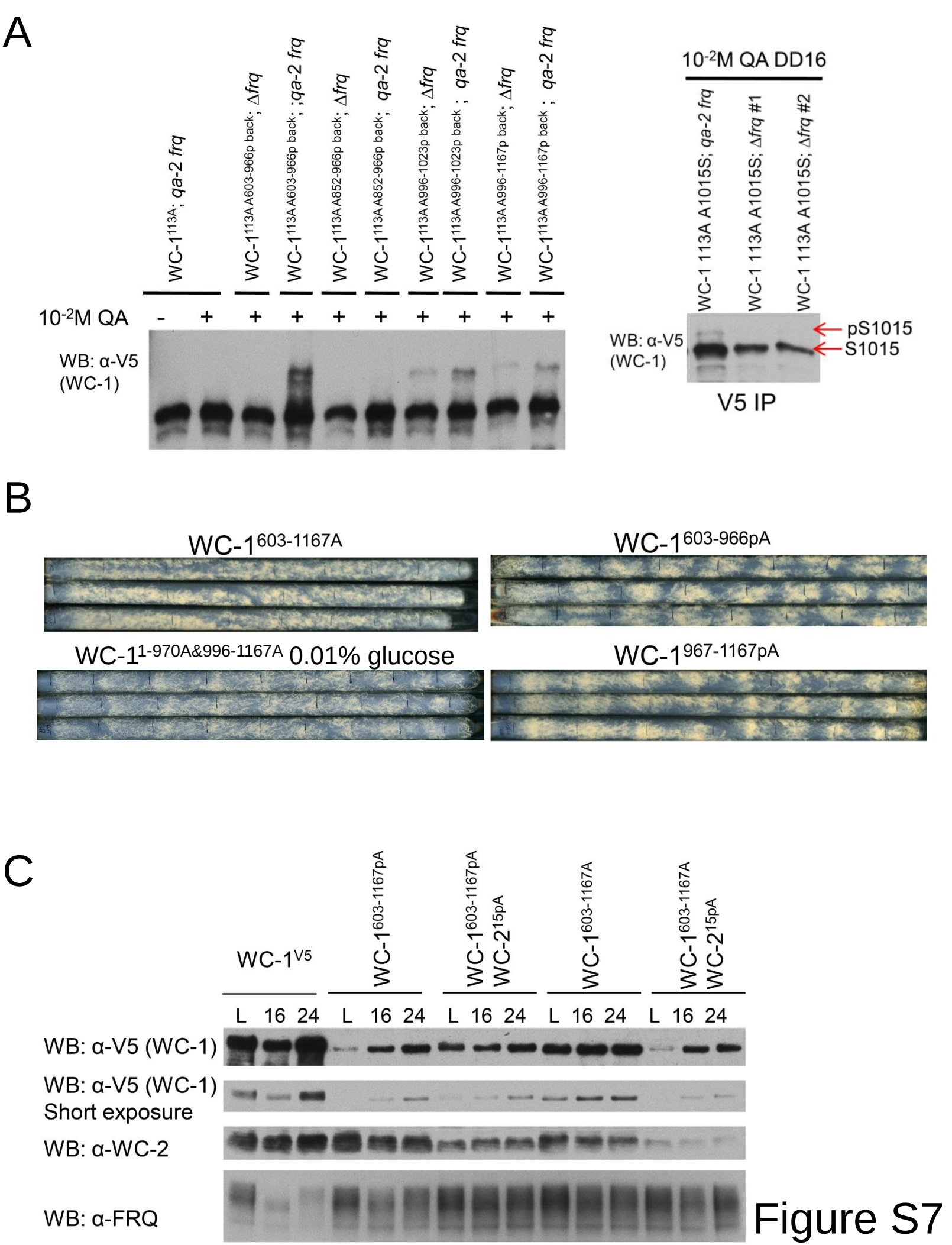
A
WC-1^113A; qa-2 frq
WC-1^113A A603-966p back; Δfrq
WC-1^113A A603-966p back; ;qa-2 frq
WC-1^113A A852-966p back; Δfrq
WC-1^113A A852-966p back; qa-2 frq
WC-1^113A A996-1023p back; Δfrq
WC-1^113A A996-1023p back ; qa-2 frq
WC-1^113A A996-1167p back; Δfrq
WC-1^113A A996-1167p back ; qa-2 frq
10-2M QA - + + + + + + + + +
WB: α-V5 (WC-1)
10-2M QA DD16
WC-1 113A A1015S; qa-2 frq
WC-1 113A A1015S; Δfrq #1
WC-1 113A A1015S; Δfrq #2
WB: α-V5 (WC-1)
pS1015
S1015
V5 IP
B
WC-1603-1167A
WC-1603-966pA
WC-11-970A&996-1167A 0.01% glucose
WC-1967-1167pA
C
WC-1V5
WC-1603-1167pA
WC-1603-1167pA WC-215pA
WC-1603-1167A
WC-1603-1167A WC-215pA
L 16 24 L 16 24 L 16 24 L 16 24 L 16 24
WB: α-V5 (WC-1)
WB: α-V5 (WC-1) Short exposure
WB: α-WC-2
WB: α-FRQ

Figure S7

Figure S8

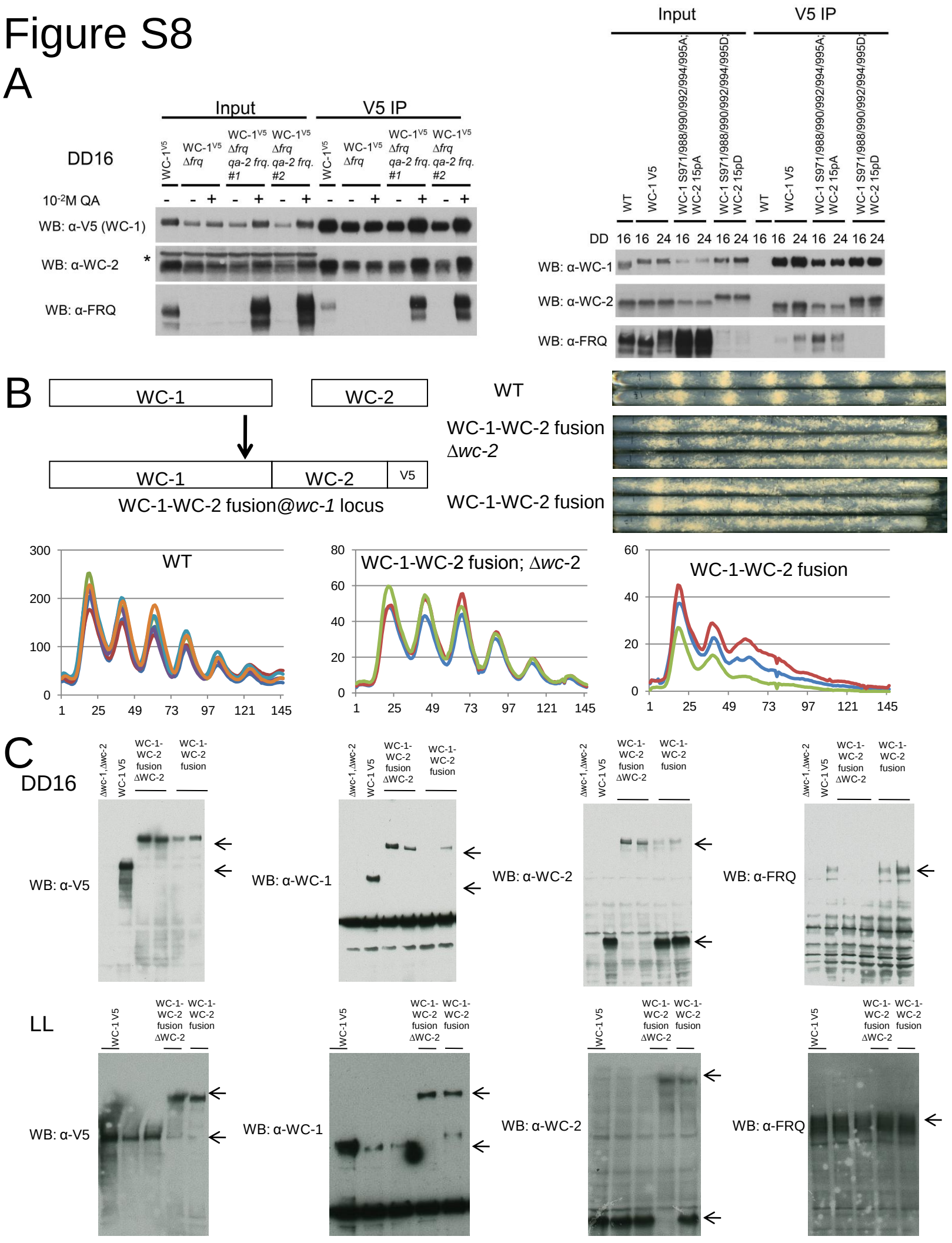
A
Input
V5 IP
DD16
WC-1V5
WC-1V5 Δfrq
WC-1V5 Δfrq qa-2 frq. #1
WC-1V5 Δfrq qa-2 frq. #2
10-2M QA
WB: α-V5 (WC-1)
WB: α-WC-2
*
WB: α-FRQ
WT
WC-1 V5
WC-1 S971/988/990/992/994/995A; WC-2 15pA
WC-1 S971/988/990/992/994/995D; WC-2 15pD
DD 16 16 24 16 24 16 24 16 16 24 16 24 16 24
WB: α-WC-1
WB: α-WC-2
WB: α-FRQ
B
WC-1
WC-2
V5
WC-1-WC-2 fusion@wc-1 locus
WT
WC-1-WC-2 fusion Δwc-2
WC-1-WC-2 fusion
WT
WC-1-WC-2 fusion; Δwc-2
WC-1-WC-2 fusion
C
DD16
Δwc-1,Δwc-2
WC-1 V5
WC-1-WC-2 fusion ΔWC-2
WC-1-WC-2 fusion
WB: α-V5
WB: α-WC-1
WB: α-WC-2
WB: α-FRQ
LL

A

NCU07024: mitogen-activated protein kinase (os-2)

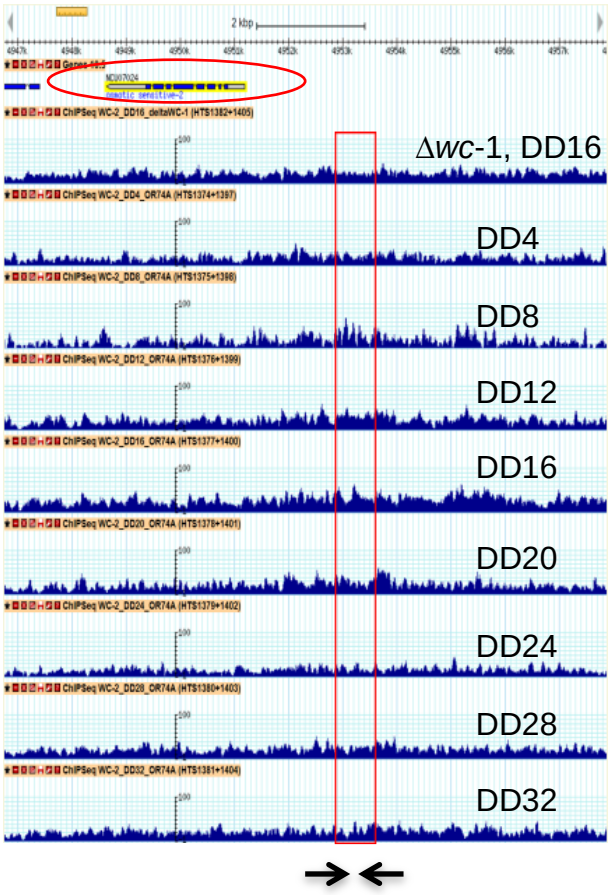

NCU01154: submerged protoperithecia-1 (sub-1)

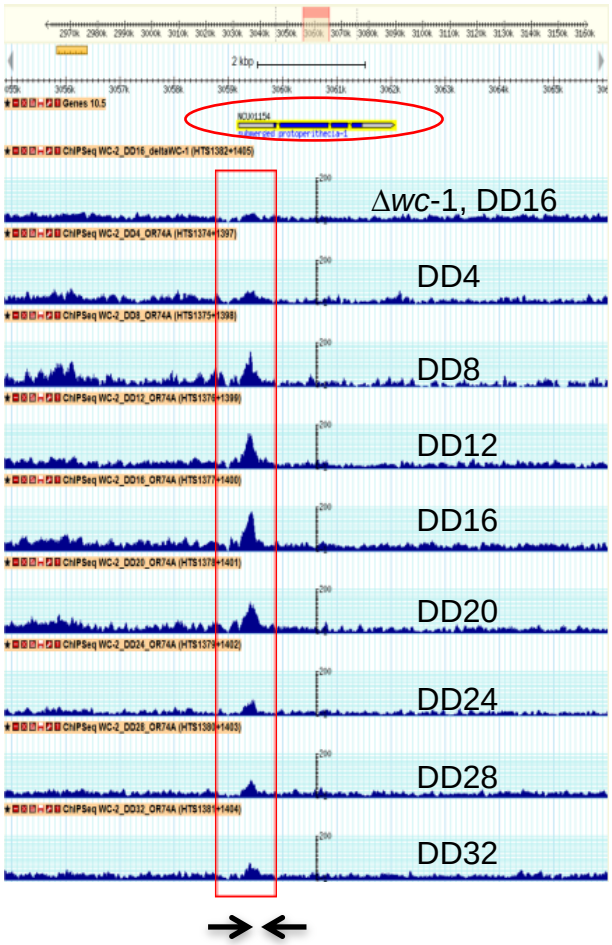

NCU02123: mitochondrial GTPase-1 (mga-1)

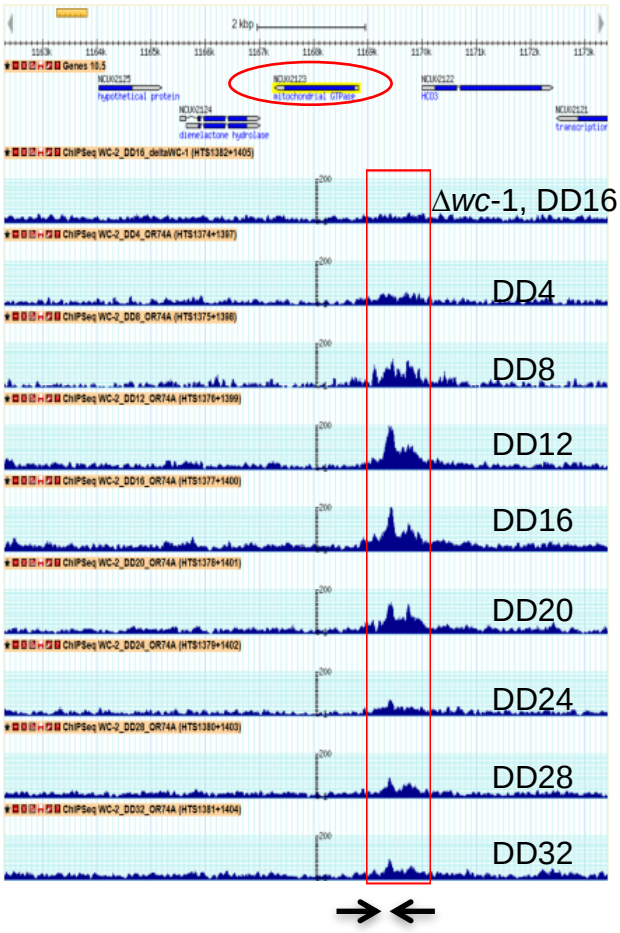

NCU02724: transcription factor-21 (tcf-21)

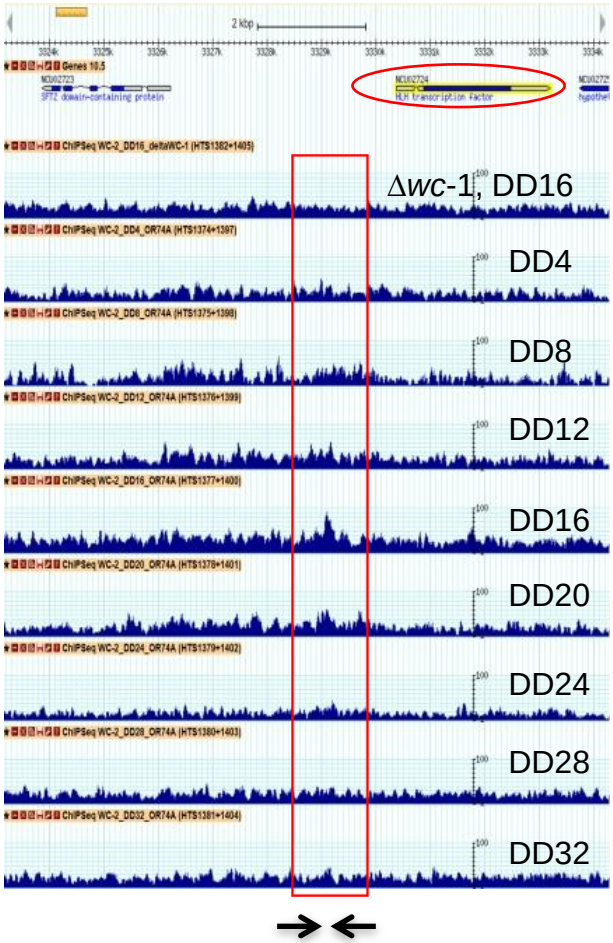

Figure S9

NCU02713: conidial separation-1 (csp-1)

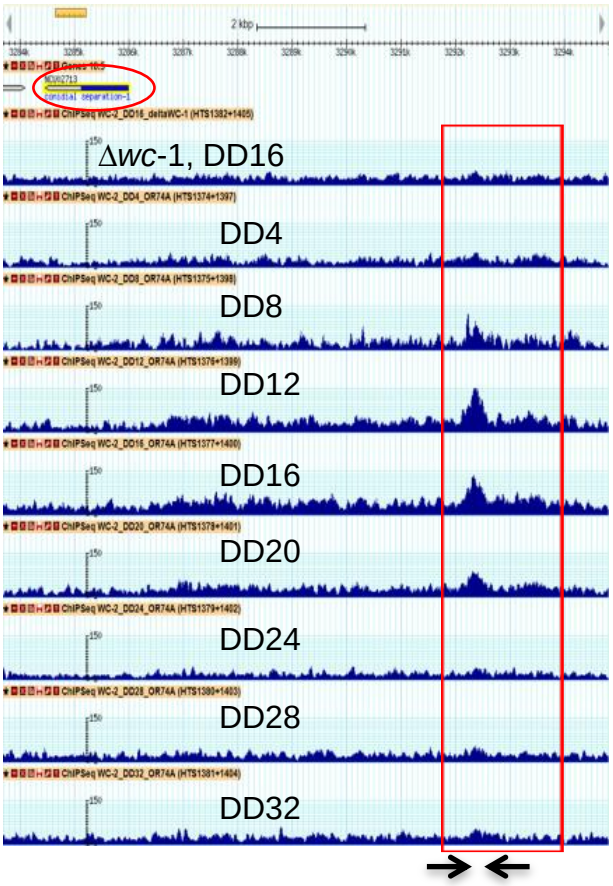

NCU02755: PAP2 domain-containing protein

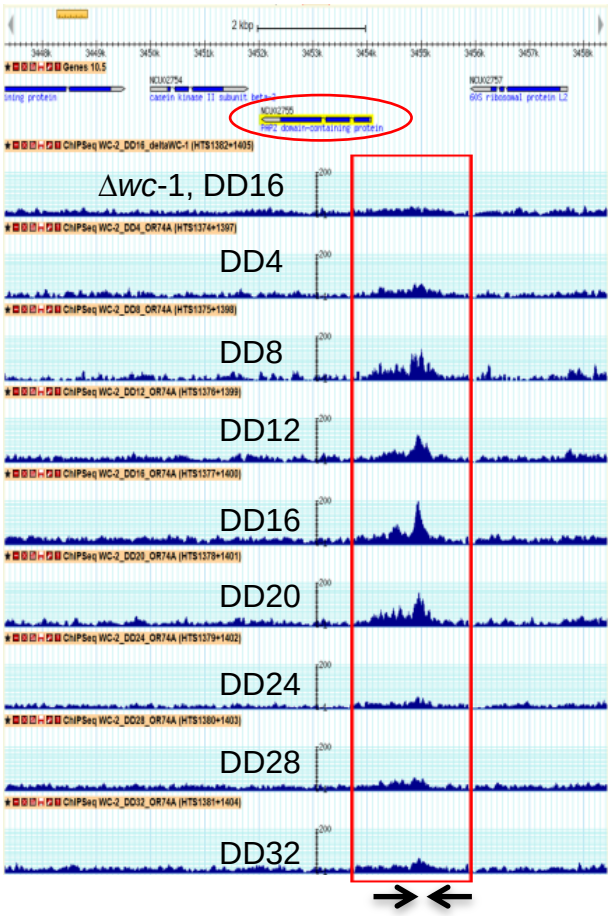

NCU03071: MAP kinase kinase kinase SskB (os-4)

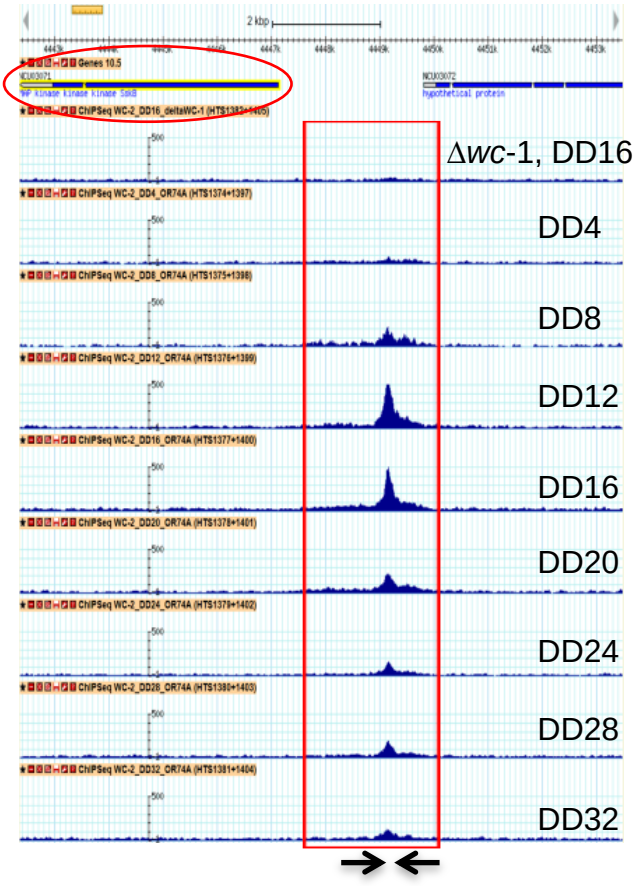

NCU03520: hypothetical protein

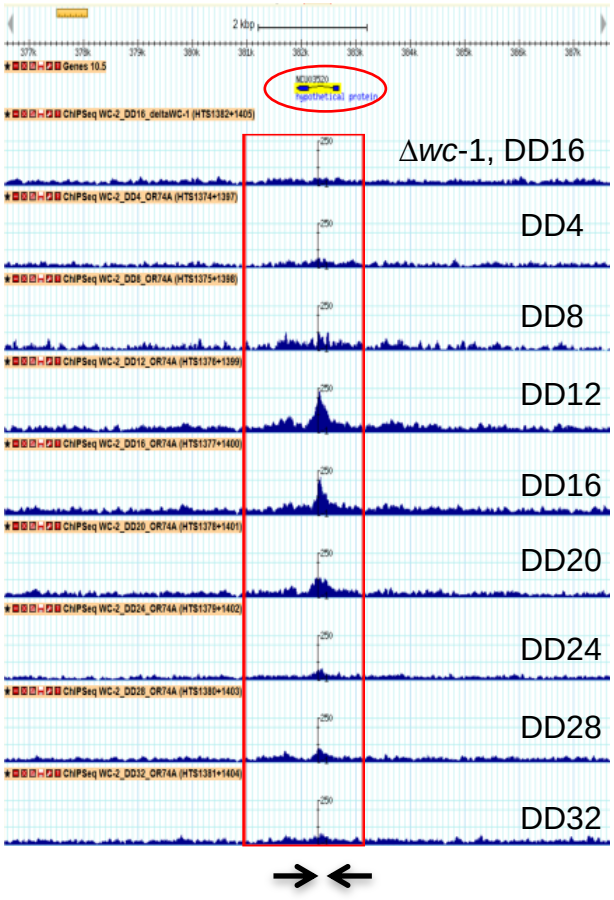

Figure S9 A continued

NCU04005: casein kinase 1b (ck-1b)

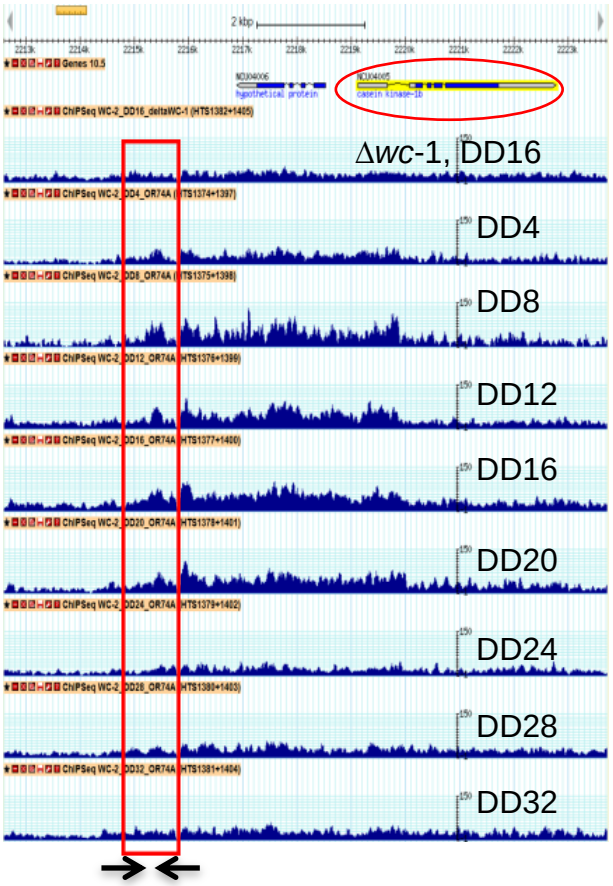

NCU08457: rodlet protein (eas)

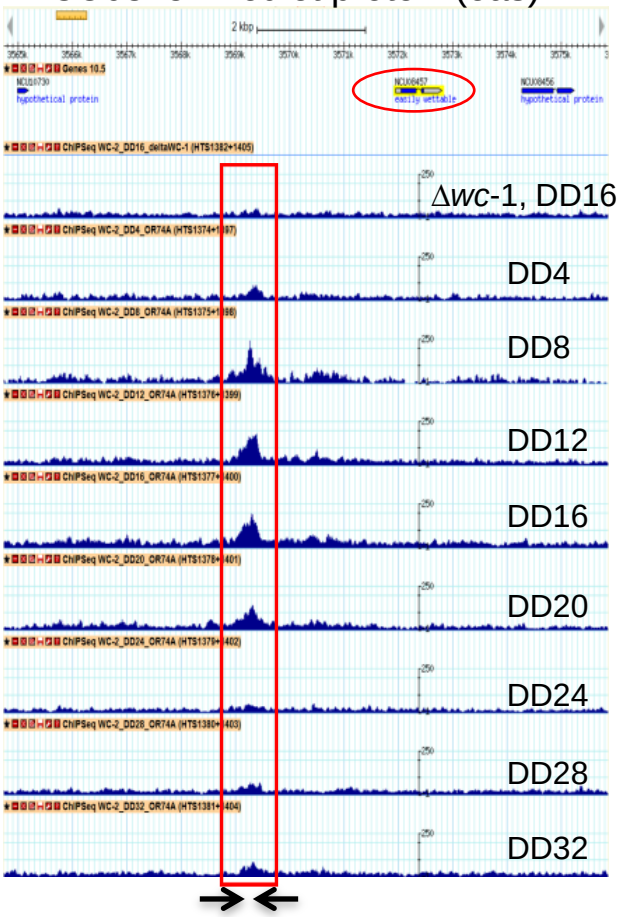

NCU11260: hypothetical protein

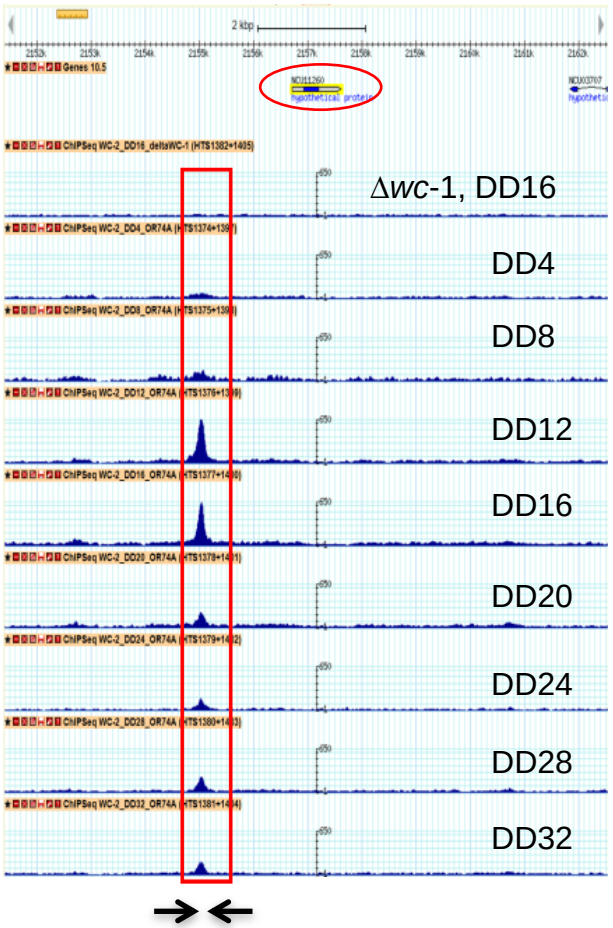

NCU06660: plasma membrane proteolipid 3 (pmp-1)

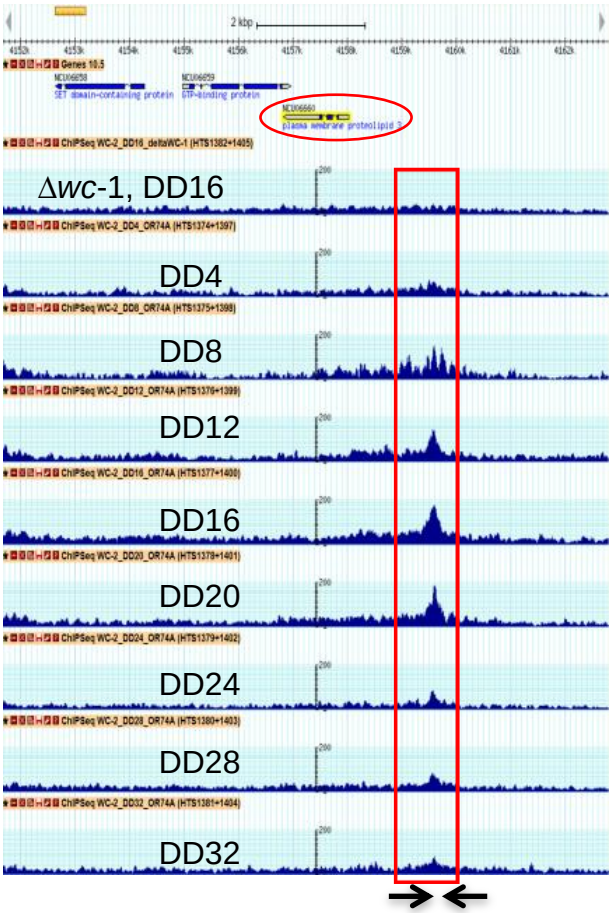

Figure S9 A continued

B

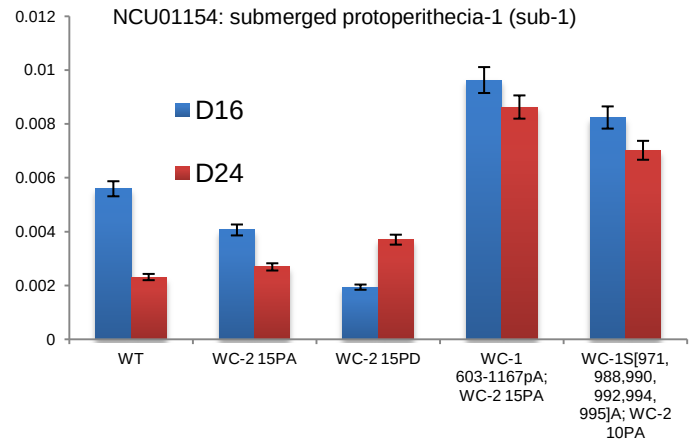
NCU01154: submerged protoperithecia-1 (sub-1)
D16
D24
0.012
0.01
0.008
0.006
0.004
0.002
0
WT
WC-2 15PA
WC-2 15PD
WC-1 603-1167pA; WC-2 15PA
WC-1S[971, 988,990, 992,994, 995]A; WC-2 10PA

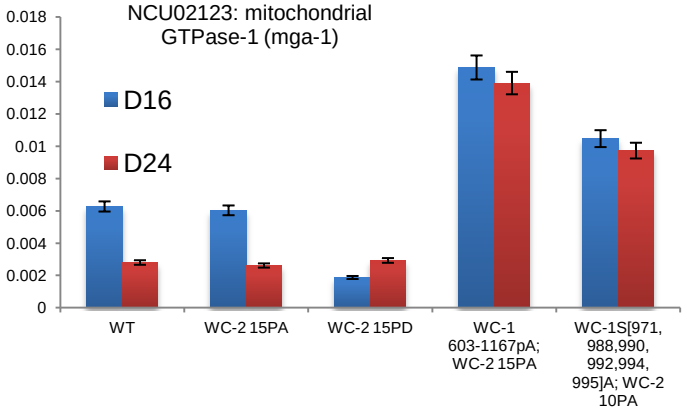
NCU02123: mitochondrial GTPase-1 (mga-1)
D16
D24
0.018
0.016
0.014
0.012
0.01
0.008
0.006
0.004
0.002
0
WT
WC-2 15PA
WC-2 15PD
WC-1 603-1167pA; WC-2 15PA
WC-1S[971, 988,990, 992,994, 995]A; WC-2 10PA

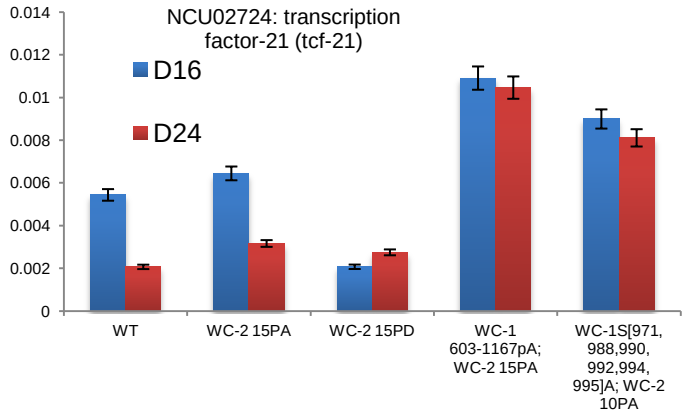
NCU02724: transcription factor-21 (tcf-21)
D16
D24
0.014
0.012
0.01
0.008
0.006
0.004
0.002
0
WT
WC-2 15PA
WC-2 15PD
WC-1 603-1167pA; WC-2 15PA
WC-1S[971, 988,990, 992,994, 995]A; WC-2 10PA

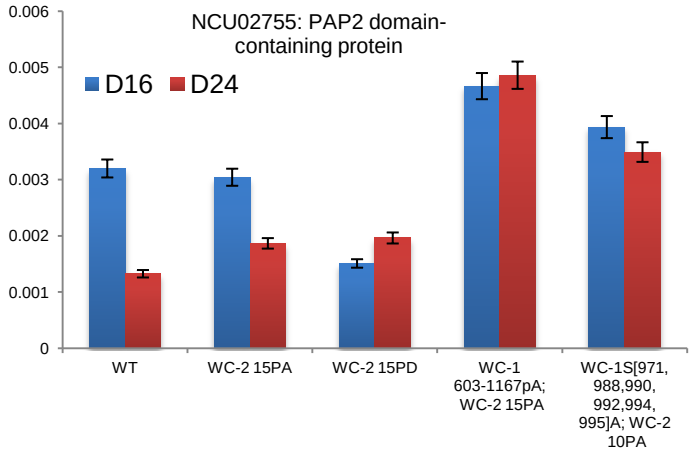
NCU02755: PAP2 domain-containing protein
D16
D24
0.006
0.005
0.004
0.003
0.002
0.001
0
WT
WC-2 15PA
WC-2 15PD
WC-1 603-1167pA; WC-2 15PA
WC-1S[971, 988,990, 992,994, 995]A; WC-2 10PA

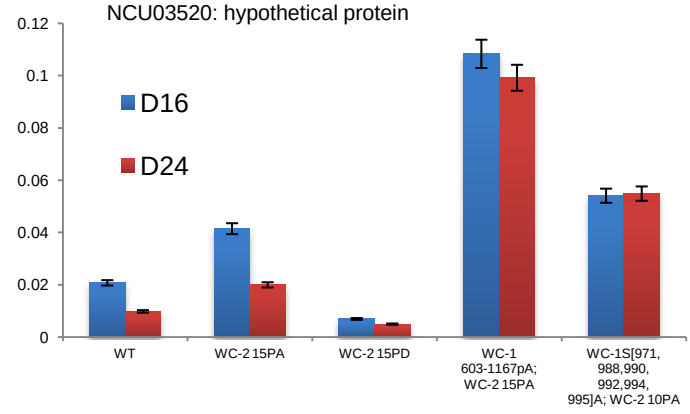
NCU03520: hypothetical protein
D16
D24
0.12
0.1
0.08
0.06
0.04
0.02
0
WT
WC-2 15PA
WC-2 15PD
WC-1 603-1167pA; WC-2 15PA
WC-1S[971, 988,990, 992,994, 995]A; WC-2 10PA

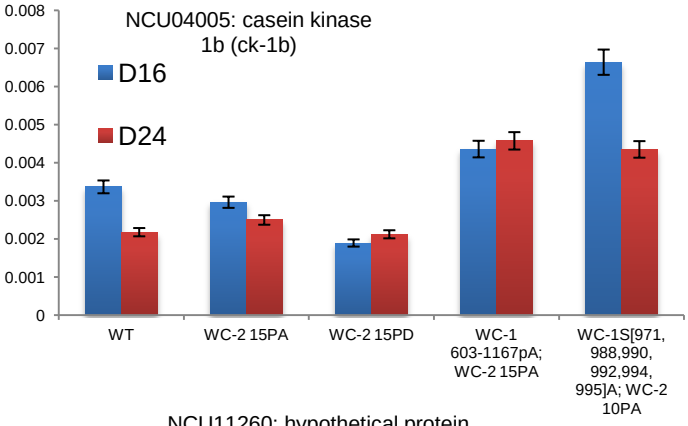
NCU04005: casein kinase 1b (ck-1b)
D16
D24
0.008
0.007
0.006
0.005
0.004
0.003
0.002
0.001
0
WT
WC-2 15PA
WC-2 15PD
WC-1 603-1167pA; WC-2 15PA
WC-1S[971, 988,990, 992,994, 995]A; WC-2 10PA

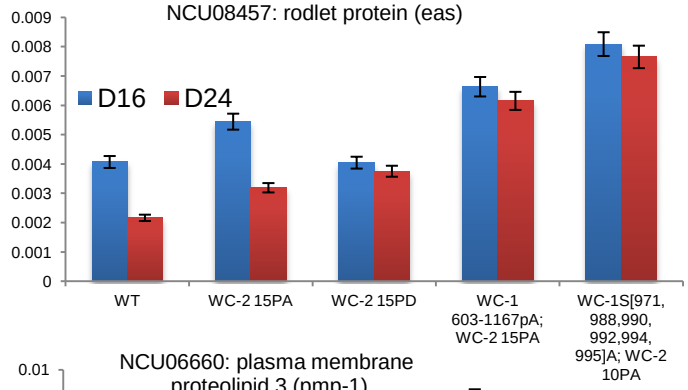
NCU08457: rodlet protein (eas)
D16
D24
0.009
0.008
0.007
0.006
0.005
0.004
0.003
0.002
0.001
0
WT
WC-2 15PA
WC-2 15PD
WC-1 603-1167pA; WC-2 15PA
WC-1S[971, 988,990, 992,994, 995]A; WC-2 10PA

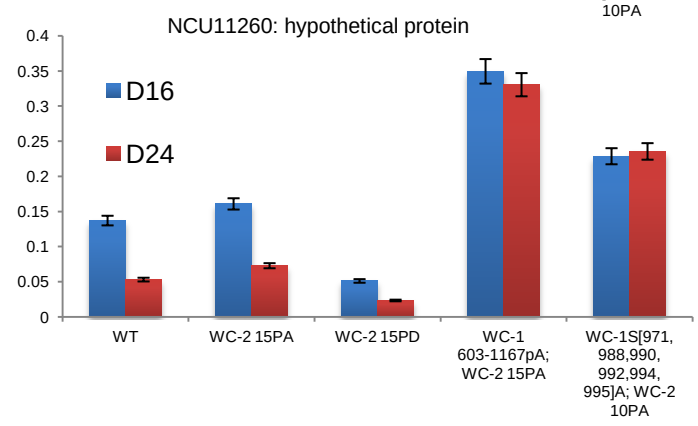
NCU11260: hypothetical protein
D16
D24
0.4
0.35
0.3
0.25
0.2
0.15
0.1
0.05
0
WT
WC-2 15PA
WC-2 15PD
WC-1 603-1167pA; WC-2 15PA
WC-1S[971, 988,990, 992,994, 995]A; WC-2 10PA

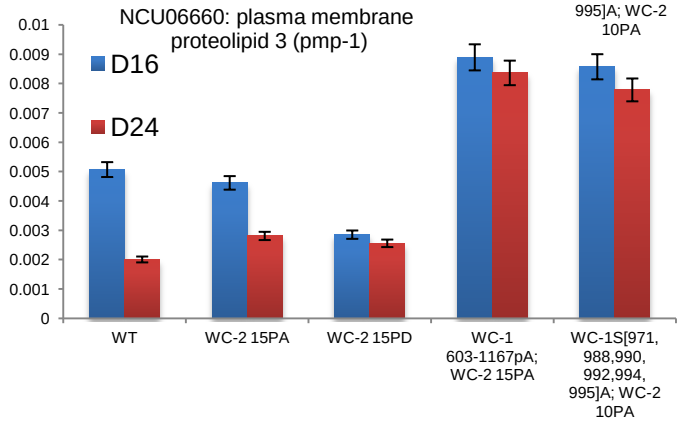
NCU06660: plasma membrane proteolipid 3 (pmp-1)
D16
D24
0.01
0.009
0.008
0.007
0.006
0.005
0.004
0.003
0.002
0.001
0
WT
WC-2 15PA
WC-2 15PD
WC-1 603-1167pA; WC-2 15PA
WC-1S[971, 988,990, 992,994, 995]A; WC-2 10PA

Figure S9

Table S1 phospho mutants race tube periods

WC-1 mutants

Sites of WC-1	Mutant I	Period	Mutant II	Period	Mutant III	Period	Mutant IV	Period	Mutant V	Period	Mutant VI	Period	Mutant VII	Period
S8	WC-1 S8A	22.4±0.0, n=3	WC-1 S8A, S11A	22.0±0.2, n=3										
S11	WC-1 S11A	22.9±0.3, n=6	WC-1 S8A, S11A	22.0±0.2, n=3										
S92	WC-1 S92A	22.6±0.3, n=6	WC-1 Δ1-100	23.0 ± 0.2, n=3										
S94	WC-1 S94A	22.7±0.2, n=3	WC-1 Δ1-100	23.0 ± 0.2, n=3										
S111	WC-1 S111A	21.5 ± 0.1, n=3	WC-1 Δ101-125	22.4 ± 0.1, n=3										
T120	WC-1 T120A	22.0 ± 0.6, n=3	WC-1 Δ101-125	22.4 ± 0.1, n=3										
S124	WC-1 S124A	21.4 ± 0.1, n=3	WC-1 Δ101-125	22.4 ± 0.1, n=3	WC-1 S124A, S200A, S234A, T238A	22.3±0.3, n=3								
Y198	WC-1 Y198A	23.2±0.0, n=3	WC-1 Δ183-200	23.7 ± 0.2, n=3										
S200	WC-1 S200A	22.9±0.4, n=3	WC-1 Δ183-200	23.7 ± 0.2, n=3	WC-1 S200A, S234A, T238A	24.7±0.6, n=3								
T214	WC-1 Δ201-300	21.8 ± 0.4, n=3												
T217	WC-1 Δ201-300	21.8 ± 0.4, n=3												
S220	WC-1 Δ201-300	21.8 ± 0.4, n=3												
S227	WC-1 S227A	21.4 ± 0.1, n=6	WC-1 Δ201-300	21.8 ± 0.4, n=3										
S229	WC-1 S229A	21.0±0.0, n=2	WC-1 S229A, S231A	21.6±0.4, n=3	WC-1 Δ201-300	21.8 ± 0.4, n=3								
S231	WC-1 S231A	21.6±0.1, n=3	WC-1 S229A, S231A	21.6±0.4, n=3	WC-1 Δ201-300	21.8 ± 0.4, n=3								
S234	WC-1 S234A	22.0±0.1, n=3	WC-1 Δ201-300	21.8 ± 0.4, n=3	WC-1 S200A, S234A, T238A	24.7±0.6, n=3								
T238	WC-1 T238A	22.9±0.2, n=3	WC-1 Δ201-300	21.8 ± 0.4, n=3	WC-1 S200A, S234A, T238A	24.7±0.6, n=3								
S264	WC-1 S264A	22.4±0.4, n=3	WC-1 Δ201-300	21.8 ± 0.4, n=3										
T275	WC-1 T275A	22.4±0.4, n=3	WC-1 Δ201-300	21.8 ± 0.4, n=3										
T279	WC-1 T279A	22.6±0.3, n=6	WC-1 Δ201-300	21.8 ± 0.4, n=3										
T287	WC-1 T287A	21.5 ± 0.4, n=3	WC-1 Δ201-300	21.8 ± 0.4, n=3										
S302	WC-1 S302A	21.3 ± 0.1, n=3	WC-1 Δ301-350	22.3±0.3, n=5										
S307	WC-1 S307A	22.1±0.2, n=2	WC-1 Δ301-350	22.3±0.3, n=5	WC-1 S307A, T308A, S315A	22.7±0.0, n=2								
T308	WC-1 T308A	22.3±0.0, n=3	WC-1 Δ301-350	22.3±0.3, n=5	WC-1 S307A, T308A, S315A	22.7±0.0, n=2								
T311	WC-1 T311A	21.6±0.5, n=3	WC-1 Δ301-350	22.3±0.3, n=5										
T312	WC-1 Δ301-350	22.3±0.3, n=5												
S315	WC-1 S315A	22.3±0.2, n=3	WC-1 Δ301-350	22.3±0.3, n=5	WC-1 S307A, T308A, S315A	22.7±0.0, n=2	WC-1 S315A, S319A	21.8±0.2, n=3						
S319	WC-1 S319A	22.5±0.5, n=3	WC-1 Δ301-350	22.3±0.3, n=5	WC-1 S315A, S319A	21.8±0.2, n=3								
T321	WC-1 Δ301-350	22.3±0.3, n=5												
T324	WC-1 Δ301-350	22.3±0.3, n=5												
S334	WC-1 S334A	21.7±0.7, n=2	WC-1 Δ301-350	22.3±0.3, n=5	WC-1 S334A, T340A	21.3±0.2, n=3								
T336	WC-1 S336A	22.3±0.7, n=3	WC-1 Δ301-350	22.3±0.3, n=5										
T340	WC-1 T340A	22.3±0.3, n=3	WC-1 Δ301-350	22.3±0.3, n=5	WC-1 S334A, T340A	21.3±0.2, n=3								
T345	WC-1 T345A, S346A, T347A	21.6±0.2, n=6	WC-1 Δ301-350	22.3±0.3, n=5										
S346	WC-1 T345A, S346A, T347A	21.6±0.2, n=6	WC-1 Δ301-350	22.3±0.3, n=5										
T347	WC-1 T345A, S346A, T347A	21.6±0.2, n=6	WC-1 Δ301-350	22.3±0.3, n=5										
S349	WC-1 Δ301-350	22.3±0.3, n=5												
S363	WC-1 S363A	22.4±0.0, n=3	WC-1 Δ351-363	21.7±0.1, n=3										
Y373	WC-1 Δ364-388	Arr. n=3	WC-1 Δ351-363	21.7±0.1, n=3										
Y525	WC-1 Y525A	25.5±0.0, n=2												
T526	WC-1 T526A	23.2±0.3, n=3	WC-1 T526A, S528A	22.9±0.1, n=3										
S528	WC-1 S528A	22.6±0.4, n=3	WC-1 T526A, S528A	22.9±0.1, n=3										
T536	WC-1 T536A	21.3±0.3, n=6	WC-1 T536A, P537A, P538A, T539A, Q540A (A536-540)	20.6±0.4, n=4										
S602	WC-1 32PA	22.3±0.2, n=3												
S748	WC-1 K746A, E747A, S748A, R749A (A746-750)	24.2±0.6, n=3												
T755	WC-1 E751A, F752A, G753A, R754A, T755A (A751-755)	25.3±0.5, n=3												
S809	WC-1 S809A	22.1±0.1, n=3												
T819	WC-1 T819A	21.8±0.2, n=3	WC-1 Δ804-820	23.7±0.4, n=3										
S824	WC-1 S824A	21.7±0.1, n=3	WC-1 S824A, S831A	21.6±0.2, n=3										
S831	WC-1 S831A	22.5±0.3, n=3	WC-1 S824A, S831A	21.6±0.2, n=3										
T838	WC-1 Δ821-857	22.4±0.1, n=3												
S840	WC-1 S840A	22.5±0.2, n=3	WC-1 Δ821-857	22.4±0.1, n=3										
S842	WC-1 S842A	22.0±0.1, n=3	WC-1 Δ821-857	22.4±0.1, n=3										
S852	WC-1 S852A	22.6±0.5, n=3	WC-1 S852A, S854A	21.5±0.1, n=3	WC-1 Δ821-857	22.4±0.1, n=3								

Continued

Sites of WC-1	Mutant I	Period	Mutant II	Period	Mutant III	Period	Mutant IV	Period	Mutant V	Period	Mutant VI	Period	Mutant VII	Period
S854	WC-1 S854A	22.6±0.1, n=6	WC-1 S852A, S854A	21.5±0.1, n=3	WC-1 Δ821-857	22.4±0.1, n=3								
S855	WC-1 S855A	21.8±0.1, n=3	WC-1 S855A, S857A	21.3±0.2, n=3	WC-1 Δ821-857	22.4±0.1, n=3								
S857	WC-1 S857A	22.1±0.4, n=3	WC-1 S855A, S857A	21.3±0.2, n=3	WC-1 Δ821-857	22.4±0.1, n=3								
T858	WC-1 Δ858-883	22.7±0.1, n=3												
S863	WC-1 Δ858-883	22.7±0.1, n=3												
S866	WC-1 S866A	22.7±0.2, n=3	WC-1 Δ858-883	22.7±0.1, n=3										
S867	WC-1 S867A	22.3±0.0, n=3	WC-1 Δ858-883	22.7±0.1, n=3										
S892	WC-1 R889L, T891A, S892A, Y895F, R898L	25.0±0.1, n=2	WC-1 32PA	22.3±0.2, n=3										
S971	WC-1 S971A	20.4±0.3, n=2												
S985	WC-1 Δ983-1011	20.2±0.3, n=3												
S988	WC-1 S988A	22.0±0.1, n=3	WC-1 Δ983-1011	20.2±0.3, n=3	WC-1 S988A, S994A	20.9±0.0, n=3	WC-1 S988A, S995A	21.6±0.4, n=3	WC-1 S988A, S990A	19.7±0.1, n=3	WC-1 S988A, S992A	20.8±0.1, n=3	WC-1 S988A, S990A, S992A, S994A, S995A	20.1±0.4, n=3
S990	WC-1 S990A	20.3±0.1, n=3	WC-1 Δ983-1011	20.2±0.3, n=3	WC-1 S990A, S992A	19.6±0.5, n=3	WC-1 S990A, S994A	19.6±0.1, n=3	WC-1 S988A, S990A	19.7±0.1, n=3	WC-1 S990A, S995A	19.9±0.9, n=3	WC-1 S988A, S990A, S992A, S994A, S995A	20.1±0.4, n=3
S992	WC-1 S992A	22.7±0.1, n=3	WC-1 Δ983-1011	20.2±0.3, n=3	WC-1 S990A, S992A	19.6±0.5, n=3	WC-1 S988A, S992A	20.8±0.1, n=3	WC-1 S992A, S994A	21.2±0.0, n=2	WC-1 S988A, S990A, S992A, S994A, S995A	20.1±0.4, n=3		
S994	WC-1 S994A	21.6±0.2, n=3	WC-1 Δ983-1011	20.2±0.3, n=3	WC-1 S988A, S994A	20.9±0.0, n=3	WC-1 S990A, S994A	19.6±0.1, n=3	WC-1 S992A, S994A	21.2±0.0, n=2	WC-1 S994A, S995A	21.3±0.1, n=3	WC-1 S988A, S990A, S992A, S994A, S995A	20.1±0.4, n=3
S995	WC-1 S995A	21.9±0.2, n=3	WC-1 Δ983-1011	20.2±0.3, n=3	WC-1 S990A, S995A	19.9±0.9, n=3	WC-1 S988A, S995A	21.6±0.4, n=3	WC-1 S994A, S995A	21.3±0.1, n=3	WC-1 S988A, S990A, S992A, S994A, S995A	20.1±0.4, n=3		
S1005	WC-1 S1005A	22.7±0.5, n=3	WC-1 Δ983-1011	20.2±0.3, n=3	WC-1 S1005A, T1012A	21.9±0.3, n=3								
S1007	WC-1 Δ983-1011	20.2±0.3, n=3												
T1008	WC-1 Δ983-1011	20.2±0.3, n=3												
T1009	WC-1 Δ983-1011	20.2±0.3, n=3												
T1012	WC-1 T1012A	21.8±0.4, n=3	WC-1 S1005A, T1012A	21.9±0.3, n=3	WC-1 Δ1012-1040	22.3±0.3, n=3								
S1015	WC-1 S1015A, S1017A	22.0±0.1, n=3												
S1017	WC-1 S1015A, S1017A	22.0±0.1, n=3												
S1021	WC-1 Δ1012-1040	22.3±0.3, n=3												
T1023	WC-1 Δ1012-1040	22.3±0.3, n=3												
T1068	WC-1 Δ1041-1074	22.5±0.2, n=3												
S1071	WC-1 S1071A	22.9±0.0, n=3	WC-1 Δ1041-1074	22.5±0.2, n=3										
S1074	WC-1 S1071A, S1074A	22.0±0.0, n=3	WC-1 Δ1041-1074	22.5±0.2, n=3										
S1134	WC-1 Δ1083-1167	22.4±0.2, n=3												
S1142	WC-1 S1142A	22.9±0.1, n=3	WC-1 Δ1083-1167	22.4±0.2, n=3										

WC-2 mutants

Sites of WC-2	Mutant I	Period	Mutant II	Period
S82	WC-2 S82A	22.1±0.2, n=3		
S118	WC-2 4+15A	21.6±0.1, n=3	WC-2 4+15A	21.6±0.1, n=3
T136	WC-2 T136A	22.9±0.5, n=3		
S233	WC-2 S233A, R236A, Y239A, R240A, R242A, K243A, K244A	22.4±0.2, n=2		
S324	WC-2 S324A, H325A, R326A, T327A, R329A, S331A, R335A, S336A	25.4±0.3, n=3		
S331	WC-2 S324A, H325A, R326A, T327A, R329A, S331A, R335A, S336A	25.4±0.3, n=3		
T339	WC-2 T339A	22.6±0.2, n=3		
S341	WC-2 S341A, S344A	22.3±0.1, n=3	WC-2 S341A, T344A, T346A, T351A, Y354A	23.2±0.8, n=3
T344	WC-2 S341A, S344A	22.3±0.1, n=3	WC-2 S341A, T344A, T346A, T351A, Y354A	23.2±0.8, n=3
T346	WC-2 S341A, T344A, T346A, T351A, Y354A	23.2±0.8, n=3		
S394	WC-2 S394A	21.5±0.2, n=3	WC-2 S390A, R391A, S394A, R396A, K398A, R401A, Y402A	21.8±0.5, n=3
T428	WC-2 T428A	25.8±0.2, n=2		
T429	WC-2 T429A	23.4±0.2, n=2		
S433	WC-2 S433A	21.4±0.2, n=3		
T435	WC-2 S435A	22.5±0.7, n=3		

WC-1 1-970A&996-1167A

Mutant I	Period
WC-1$^{1\text{-}970A\&996\text{-}1167A}$	23.5±0.4, n=3

Table S3 Potential kinase prediction for key sites on the WCC

Amino acid	Period (to A) by race tube	Predicted Kinase by KinasePhos (90% Prediction Specificity)
WC-1 S971	20.4±0.3, n=2	PKC, CaM-II, PKG, cdc2, MAPK, CDK
WC-1 S988	22.0±0.1, n=3	PKG, IKK
WC-1 S990	20.3±0.1, n=3	PKA, PKG, CKI, cdc2, MAPK, CDK, ATM, IKK
WC-1 S992	22.7±0.1, n=3	CKI, CKII, CDK, cdc2, ATM, IKK
WC-1 S994	21.6±0.2, n=3	CKI, ATM, PKA
WC-1 S995	21.9±0.2, n=3	CDK, cdc2
WC-2 S331	25.4±0.3, n=3 (WC-2$^{S324A, H325A, R326A, T327A, R329A, S331A, R335A, S336A}$)	PKG
WC-2 T339	22.6±0.2, n=3	MAPK, CDK
WC-2 S341	22.3±0.1, n=3 (WC-2$^{S341A, S344A}$)	CKII, ATM, MAPK
WC-2 S433	21.4±0.2, n=3	CaM-II, cdc2, CDK
WC-2 T435	22.5±0.7, n=3	PKC

Table S4 Circadian period of the *wcc* mutants as reported by the *frq* promoter-driven *luciferase* gene assay

Mutant	Period	Phase
WT (661-4a)	21.2±0.4, n=3	19.3±0.5, n=3
wc-1^{113A}	arr	NA
wc-1^{80A}	arr.	NA
wc-1$^{1\text{-}602A}$	arr	NA
wc-1$^{1\text{-}602A,\ A363S,\ A373Y,\ A390S,\ A525Y}$	22.7±0.1, n=3	20.6±0.5, n=3
wc-1$^{1\text{-}602pA}$	arr	NA
wc-1$^{1\text{-}602pA,\ A363S,\ A373Y,\ A525Y}$	19.4±1.9, n=3	19.6±1.1, n=3
wc-1$^{603\text{-}1167A}$	22.8±0.1, n=3	20, n=3
wc-1$^{603\text{-}1167pA}$	21.6±1.6, n=3	19±1.7, n=3
wc-1$^{603\text{-}966A}$	20.8±0.1, n=3	16, n=3
wc-1$^{603\text{-}966pA}$	20.8±0.1, n=3	19, n=3
wc-1$^{967\text{-}1167A}$	21.9±0.2, n=3	18, n=3
wc-1$^{967\text{-}1167pA}$	19.0±0.5, n=3	17.6±0.5, n=3
wc-1$^{967\text{-}1023pA}$	19.2±0.4, n=3	16.6±0.5, n=3
wc-1$^{1023\text{-}1167pA}$	21.6±0.2, n=3	20±1, n=3
wc-1$^{1023\text{-}1167pA}$; *wc*-2^{15pA}	20.6±0.5, n=3	18.6±1.1, n=3
wc-1$^{S971A,\ S988A,\ S990A,\ S992A,\ S994A,\ S995A}$	19.1±0.1, n=3	14.3±0.5, n=3
wc-1$^{S971D,\ S988D,\ S990D,\ S992D,\ S994D,\ S995D}$	23.6±0.7, n=3	20±1.7, n=3
wc-1$^{S971A,\ S990A}$	19.7±0.1, n=3	16.6±0.5, n=3
wc-2^{15pA}	20.2±0.2, n=3	16.6±0.5, n=3
wc-2^{12pA}	21.2±0.4, n=3	19.3±0.5, n=3
wc-2^{11pA}	20.7±0.1, n=3	18, n=3
wc-2^{10pA}	20.6±0.2, n=3	19, n=3
wc-2^{9pA}	20.3±0.6, n=3	19, n=3
wc-2^{8pA}	21.2±0.5, n=3	18.3±0.5, n=3
wc-2^{7pA}	20.6±0.4, n=3	18, n=3
wc-2^{6pA}	20.9±0.3, n=3	19, n=3
wc-2 $^{S331A,\ S339A,\ S341A,\ S344A,\ S346A}$	21.7±0.6, n=3	19, n=3
wc-1$^{S971A,\ S988A,\ S990A,\ S992A,\ S994A,\ S995A}$; *wc*-2 $^{S331A,\ S339A,\ S341A,\ S344A,\ S346A}$	22.5±0.2, n=3	19±2, n=3
wc-2 $^{S394A,\ S428A,\ S429A,\ S433A,\ S435A}$ (*wc*-2^{5pA})	20.2±0.1, n=3	18.3±0.5, n=3
wc-1$^{S971A,\ S988A,\ S990A,\ S992A,\ S994A,\ S995A}$; *wc*-2 $^{S394A,\ S428A,\ S429A,\ S433A,\ S435A}$ (*wc*-2^{5pA})	18.4±0, n=3	16.3±2.3, n=3
wc-1-wc-2 fusion; ∆wc-2	23.0±0.7, n=3	21.3±0.5, n=3
wc-1-wc-2 fusion	20.8±0.4, n=3	18, n=3

Table S5 Primers sets used in Figure 5 and Figure S6

Primer name	Primer sequence	Target gene
1154qChipF	ACT TGT TAC CTG ACC GGA CC	*ncu01154*
1154qChipR	GCC ACA CCT CAG GTT ATG GGA GAT	
2123qchipsF	CGT GCC ACC ACT GTC TTT GAT	*ncu2123*
2123qchipsR	ACA AAC GAG AAG CGG GCA ATG G	
2713qChip sF	GTC GGC TGT CAG AGT GAT TG	*ncu02713*
2713qChip lR	GTC AAT CAG GGT CTC GAT GC	
2724qChipF	GGT GGG ACG GTT TTC ACC TCT	*ncu02724*
2724qChipR	ACT TCC GAC GAT CAG AGA AGT GC	
2755qChipF	GAC TGG GGT TCC ACT TGG CTA	*ncu02755*
2755qChipR	TGG CAT GCC GGT TGA GGT T	
3071qChipF	TGT GGT CAA GTG CGT TGA TGG	*ncu03071*
3071qChipR	AGC GCC CAA GAT CTC AAT TCT GTA G	
3520qchipF	AGA AGA GGA CGT CGA GAG TGG	*ncu03520*
3520qChipR	AAG AGT GGA TCC TCT GGT GGT C	
4005 qChipF	AAT CCG GCA TTT CCC ACA ATC TCG	*ncu04005*
4005 qChipR	CCG GGG GAA ATA GCG TTA TAA GT	
6593qChipF	GAC CGA GAA CCG ATA TCT ACC T	*ncu06593*
6593qChipsR	GGC AGA TTC ATT CTA CAC AGT CCG	
6660qchipF	AAG TAC TAT CGC GCT TCG CCT AGA	*ncu06660*
6660qchipR	GAA GGC CCA GAA GGC TCA GCT A	
7024qchipF	TAC TCG ATC AAA GTC CGA TTG CAC	*ncu07024*
7024qchipR	TTC GCA AGC CAT CGC AAG CCA T	
8457qchipF	AGG GTC TAG GCA AAC ACG GTG TCA	*ncu08457*
8457qchipR	TCC AAT CGT CTG ATC CCC CAT TCT	
11260qChipF	GAT GCA AGG TGG TCT GGA AAT G	*ncu011260*
11260qchipR	CAA GAC AGT CCA GAA CGC TG	
C box F	TCAAGTCAAGCTCGTACCCACATC	*C box of ncu02265 (frq)*
C box R	CAATTTTGCAGCGTCATCGGTCT	
pLRE F	GCTGGTCATCTCCTCAGCATTTTGTC	*pLRE of ncu02265 (frq)*
pLRE R	ATACTTGTAGGCCCGCTCCCCATC	